Accepted Manuscript

Geological Society, London, Special Publications

Visean high-K mafic-intermediate plutonic rocks of the Ossa-Morena Zone (SW Iberia): implications for regional extensional tectonics

M. Francisco Pereira, Ícaro Dias da Silva, Cármen Rodríguez, Fernando Corfu & António Castro

DOI: https://doi.org/10.1144/SP531-2022-118

To access the most recent version of this article, please click the DOI URL in the line above. When citing this article please include the above DOI.

Received 8 April 2022
Revised 11 July 2022
Accepted 11 July 2022

Supplementary material at https://doi.org/10.6084/m9.figshare.c.6243822

Visean high-K mafic-intermediate plutonic rocks of the Ossa-Morena Zone (SW Iberia): implications for regional extensional tectonics

M. Francisco Pereira[1*], Ícaro Dias da Silva[2], Cármen Rodríguez[3], Fernando Corfu[4], António Castro[3]

[1]Departamento de Geociências, Instituto de Ciências da Terra, ECT, Universidade de Évora, Apt. 94, 7002-554 Évora, Portugal; mpereiraevora.pt

[2] Faculdade de Ciências, Instituto Dom Luiz, Universidade de Lisboa, Campo Grande, Edif. C1, Piso 1, 1749-016 Lisboa, Portugal, ipicaparopo@gmail.com

[3]Instituto Andaluz de Ciencias de la Tierra (IACT). Consejo Superior de Investigaciones Científicas- Universidad de Granada 18100 Armilla, Granada, Spain; carmenrdealmodovar@gmail.com; antonio.castro@csic.es

[4] Department of Geosciences and CEED, University of Oslo, Oslo, Norway, fernando.corfu@geo.uio.no

*****Correspondence: mpereira@evora.pt

Abstract

Field relationships and new U-Pb geochronology data indicate a temporal link among the diverse high-K mafic-intermediate magmas of the Ossa-Morena Zone (OMZ). Ages of ca. 338-335 Ma for the Vale de Maceiras gabbro and the Campo Maior microdiorite and quartz-diorite indicate that plutonism took place during Variscan extensional D_2 deformation event in the OMZ. The syn-tectonic nature of the Vale de Maceiras pluton is attested by the orientation of intrusive contacts, magmatic foliation, and growth of contact metamorphic minerals in relation to Variscan extensional D_2 foliation. The Campo Maior microdiorite, quartz-diorite, and orthomigmatites are temporally linked to high-temperature mylonitic gneisses formed simultaneously with the Variscan extensional D_2 deformation event. The geochemical features of the Vale de Maceiras and Campo Maior mafic-intermediate rocks show an affinity with the sanukitoid series. This finding suggests that the observed geochemical variability, from tholeiitic to calc-alkaline and sanukitoid, in the Visean OMZ plutonic rocks (ca. 349-335 Ma) may have been inherited from partially melted mantle domains that were previously contaminated by crustal melts during subduction.

Keywords: Early Carboniferous; high-K mafic-intermediate plutonism; Gondwana margin; extensional tectonics; wrenching tectonics.

Introduction

Recent petrological and geochronological studies of plutonic rocks have resulting in a better understanding of the evolution of Late Paleozoic synorogenic magmatism in SW Iberia (Castro, 2019, and references therein). Topics that have received specific attention include the to subduction polarity and the closure of oceanic basins during the collision between Gondwana and Laurussia (Ribeiro et al., 2007; Martínez-Catalán et al., 2007; Simancas et al., 2009; Pereira et al., 2017 and references therein). Progress in the knowledge of the magma sources has contributed to gradually updating the plate-tectonic models for SW Iberia (Castro et al., 1996; Simancas et al., 2009; Cambeses et al., 2015; Jesus et al., 2016; Lima et al., 2012). In this regard, the origin and tectonic significance of the early Carboniferous magmatic activity provides clues to the refinement of the models (Rodríguez et al., 2022).

In paleogeographic reconstructions for the Late Paleozoic, Iberia is placed at the core of the Pangea supercontinent as part of the west European Variscan belt, and hosts the suture zone that resulted from the closure of the Rheic Ocean as Laurussia and Gondwana collided (Matte, 1991; Quesada et al., 1994; Ribeiro et al., 2007; Simancas et al., 2009; Martínez-Catalán et al., 2021; Fig. 1a). In SW Iberia, the Late Paleozoic suture zone is defined along the boundary between the South Portuguese and Pulo do Lobo zones (SPZ and PLZ, respectively; Laurussia) and the Ossa-Morena Zone (OMZ, Gondwana) (Pereira et al., 2017 and references therein) (Fig. 1b). The Beja-Acebuches ophiolitic unit, which is located along the southern boundary of the OMZ, has been considered to trace the Rheic suture zone in this part of the Variscan belt (Quesada et al., 1994). However, the tectonic significance of the Beja-Acebuches unit, consisting of mafic-ultramafic rocks, is still under debate (Quesada et al., 1994; Azor et al., 2008; Pin and Rodríguez, 2009; Ribeiro et al., 2010; Díez Fernández et al., 2016; Pérez-Cáceres et al., 2015; Rodriguez et al., 2022).

Several plate-tectonic models have proposed oceanic lithosphere subduction to explain the origin and evolution of the Late Paleozoic synorogenic magmatism found in the OMZ, the SPZ, and the PLZ (Ribeiro et al., 1990; Castro et al., 1996; Pin et al., 2008; Jesus et al., 2016; Murphy et al., 2016; Rodriguez et al., 2022). The proposed models differ in (1) the timing of ocean closure (Late Devonian or Carboniferous?) (Azor et al., 2008; Ribeiro et al., 2010); (2) the subduction polarity and resulting onset of the magmatic arc; was the upper plate represented by Gondwana (Quesada et al., 1994; Ribeiro et al., 2007) or Laurussia (Simancas et al., 2009; Pereira et al., 2017)? and (3) the closing of a single ocean (Rheic?) or multiple oceanic basins (Rheic, Paleotethys, Rhenohercynian and/or intra-Gondwana?) (Díez Fernández et al., 2016; Pereira et al., 2017, and references therein).

In SW Iberia, the OMZ exposes sedimentary rocks and mid-crustal metamorphic rocks that were intruded by voluminous Early Carboniferous synorogenic plutonic rocks (Pereira et al., 2015; Ribeiro et al., 2019). In this study, petrography, mineral chemistry, whole-rock geochemistry, and U-Pb zircon geochronology (ID-TIMS and SHRIMP) of late Paleozoic OMZ mafic-intermediate plutonic rocks and their field relationships with metamorphic country rocks are investigated. The results contribute to a better understanding of the link between Early Carboniferous plutonism, regional tectonics, and synorogenic crustal growth in this part of the Variscan belt.

Geological setting

In SW Iberia, three main pre-Mesozoic tectonic units may be identified (Dallmeyer and Martínez Garcia, 1990): the OMZ and the Central Iberian Zone represent the Gondwana margin in the Iberian Variscan belt, the former being bounded to the south by the SPZ and the PLZ, which correspond to the Laurussia margin of the Iberian Variscan belt (Fig. 1a).

The oldest stratigraphic record of the OMZ includes Ediacaran meta-sedimentary and -igneous rocks related to a Cadomian magmatic arc (Eguíluz et al., 2000). The transition from a Neoproterozoic active continental margin to a Cambrian intracontinental rifting is marked by a regional angular discordance (Pereira et al., 2008a; Sánchez-Garcia et al., 2010). The previously deformed Ediacaran succession (Série Negra Group; Eguíluz et al., 2000; Díez Fernández et al., 2017) composed of metagreywackes, metapelites, black metacherts, and amphibolites is unconformably overlain by Cambrian-Ordovician siliciclastic and minor carbonate sequences with associated mafic and felsic volcanic rocks and is intruded by coeval plutonic equivalents (Sánchez-Garcia et al., 2010, 2013; Díez Fernández et al., 2015). Cambrian-Ordovician metamorphism is locally recognized (Sanchez-Lorda et al., 2016; Solís-Alulima et al., 2021). Silurian-Devonian OMZ stratigraphy is characterized by siliciclastic successions and the absence of magmatism. Silurian rocks include graptolitic shales and black cherts, as well as marbles at the transition with an Early Devonian sequence dominated by shales and quartzites (Terena basin; Robardet and Gutiérrez Marco, 2004). A stratigraphic hiatus is assumed to exist in the Middle Devonian. Rare Devonian limestones occur as olistoliths within Early Carboniferous synorogenic basins (Gutiérrez Marco et al., 2019 and references therein). Late Devonian stratigraphy includes shale, quartzite, and marble formations (Robardet and Gutiérrez Marco, 2004). The Early Carboniferous OMZ successions are mostly composed of siliciclastic turbidites with intercalations of felsic to mafic volcanic rocks, and minor calciturbidites (Quesada et al., 1990; Wagner, 2004). This volcano-sedimentary sequence has traditionally been interpreted to have been deposited in a collisional setting (Matachel, Peñarroya, and Santos de Maimona basins; Quesada et al., 1990). Recently, it was proposed that the Early Carboniferous OMZ turbidites may also have been deposited in a back-arc basin related to oceanic subduction acting simultaneously with the Laurussia-Gondwana convergence (Pereira et al., 2020).

SW Iberia Variscan collision has been associated with the development of a first Variscan contractional D_1 deformation phase (Ribeiro et al., 2007), evidenced by a late Devonian high-pressure metamorphic event (Moita et al., 2005a). First phase Variscan recumbent folds with a pervasive foliation developed on Cambrian-Lower Devonian sedimentary sequences are unconformably covered by the Lower Carboniferous sedimentary rocks of the Terena Basin (Quesada et al., 1990; Simancas et al., 2001). Here, these earlier Variscan structures are overprinted by upright folds formed during the second phase of Variscan contractional deformation (Simancas et al., 2001). However, the sequence of the Variscan deformation phases is controversial. Similar field relationships involving the Early Carboniferous sedimentary rocks and the foliated metamorphic basement is found in the Cabrela Basin (Quesada et al., 1990), located in the hanging-wall of the Évora gneiss dome. In this case, it was shown that the deformation of the basement rocks formed during a Variscan extensional D_2 deformation event coeval with the deposition of the Cabrela turbidites (Pereira et al., 2009, 2012, 2020; Dias da Silva et al., 2018). In the Évora gneiss dome, the Variscan contractional D_1 deformation event is difficult to recognize (Rosas et al., 2008; Dias da Silva et al., 2018) due to the overprint of the regional S_2 foliation. Finally, a second Variscan contractional deformation event was responsible for the upright folding of the Cabrela turbidites, and the development of D_3 upright folds, thrusts, and strike-slip shear zones/faults, that caused the steepening of the earlier structures (Pereira et al., 2009; Dias da Silva et al., 2018) (Fig. 2).

Along the southern boundary of the OMZ, Tournaisian gabbros and dioritic rocks of the Beja Igneous Complex (Jesus et al., 2016) (Fig. 1b), define the earliest stages of continental magmatic arc emplacement away from the continental region being exposed to the collision (Pereira et al., 2020). These authors assumed that Laurussia-Gondwana collision was primarily the result of the Rheic Ocean closure, forming a collisional orogen in the Late

Devonian. The contiguous Paleotethys Ocean started subduction beneath Gondwana (OMZ) giving birth to an accretionary orogen during the Tournaisian. Later in the Visean, the volume of arc-related plutonic rocks increased greatly and was associated with the early stages of the development of the Évora gneiss dome (Dias da Silva et al., 2018) (Fig. 1b). Variscan extensional D_2 deformation event overprint on migmatitic and plutonic rocks was heterogeneous. Intrafolial folds and pervasive S_2 foliation developed on Ediacaran and Lower Paleozoic rocks in ductile shear zones (Pereira et al., 2009; Dias da Silva et al., 2018). The footwall block of the Évora gneiss dome, composed of Variscan high-grade metamorphic rocks, is separated from the hanging-wall blocks by major extensional D_2 shear zones (Fig. 2), characterized by strong telescoping of the metamorphic gradient (Pereira et al., 2009). Visean quartz-diorites, granites, and gabbros were emplaced both in the migmatites of the footwall (Moita et al., 2009, 2015) and in the amphibolites, mica schist, and quartz-feldspathic gneisses of the hanging-wall blocks (Dias da Silva et al., 2018). Further north, along the northern boundary of the OMZ, Visean migmatitic rocks with Ediacaran and Lower Paleozoic protoliths, also occur along the Badajoz-Córdoba shear zone (Burg et al., 1981; Azor et al., 1994; Pereira et al., 2010, 2012) (Fig. 1b). Their relationship to the coeval high-grade metamorphic rocks in the Évora gneiss dome is unclear. Penetrative ductile deformation developed under high-temperature metamorphic conditions in Badajoz-Cordoba shear zone gave rise to microstructures and fabrics with kinematic criteria related to Variscan extensional tectonism (Azor et al., 1994). It is possible that the Badajoz-Cordoba shear zone acted as a Variscan extensional D_2 shear zone rather than having been a strike-slip shear zone as argued by Pereira et al. (2008b). As previously pointed out by Azor et al. (1994), this low-angle extensional shear zone was responsible for the progressive exhumation of late Devonian high-pressure metamorphic rocks (ca. 377 Ma; Abati et al., 2018), and was later folded and affected by strike-slip deformation, resulting in steepening of earlier structures (Fig. 2).

Previous geochronology

Relevant syntheses on the Late Paleozoic orogenic magmatism in SW Iberia include Sánchez Carretero et al. (1990) and Ribeiro et al. (2019). The specific case of the Late Devonian OMZ mafic plutonism in the area that has been recently studied by Lains Amaral et al. (2019) relies on absolute ages obtained with: i) Rb-Sr and K-Ar geochronology on whole rock-feldspar and amphibole from the Vale de Maceiras gabbro (weighted average age of 362 ± 13 Ma; Moita et al., 2005b); and ii) Sm-Nd geochronology on whole rock-feldspar and plagioclase from monzogabbro, anorthosite, and gabbro samples of the Campo Maior region (weighted average age of 376 ± 22 Ma; Lopes et al. 2005). However, it should be noted that the earlier geochronology K-Ar work on biotite from the Campo Maior microdiorite by Pinto Coelho et al. (1974) provided a crystallization age of 342 ± 7 Ma. The foliated migmatites, which represent the equivalent of the host rocks of the Campo Maior microdiorite and quartz-diorite, were dated at 335 ± 5 Ma (zircon U-Pb) and 334 ± 2 Ma (biotite Ar-Ar), indicating Visean ductile deformation under high-grade metamorphic conditions (Pereira et al., 2012).

U-Pb zircon crystallization ages of igneous rocks from the Évora gneiss dome and Beja Igneous Complex in Portugal (Pin et al., 2008; Pereira et al., 2015; Moita et al., 2015; Dias da Silva et al., 2018; Rodríguez et al., 2022; Pereira et al., 2022) overlap the age interval of igneous rocks from other regions of the OMZ in Spain, as the example of Acebuches, Valencia del Ventoso, Burguillos del Cierro, Santa Olalla, Brovales, Valuengo, and Cala (Montero et al., 2000; Romeo et al., 2006; Azor et al., 2008; Cambeses et al., 2015) (Fig. 1b). The igneous rocks of the Évora gneiss dome that are spatially, and most likely temporally, associated with the Vale de Maceiras and Campo Maior plutonic rocks, include: i) the Arraiolos granite (337 ± 4 Ma; U-Pb SHRIMP zircon age; Pereira et al., 2009), ii) the Almansor monzogranite-granodiorite (341 ± 2 Ma; U-Pb SHRIMP zircon age; Pereira et al., 2015), iii) the Divôr (339

± 7 Ma; U-Pb SHRIMP zircon age; Dias da Silva et al., 2018), iv) Hospitais (337 ± 2 Ma and 336.5 ± 0.5 Ma; U-Pb ID-TIMS zircon age; Moita et al., 2015), v) Reguengos de Monsaraz (337.3 ± 2.3 Ma and 337.8 ± 0.7 Ma; U-Pb ID-TIMS zircon age; Antunes et al., 2011), vi) Alto de São Bento (338 ± 3 Ma; U-Pb SHRIMP zircon age; Rodríguez et al., 2022) quartz-diorites, vii) the Alto de São Bento diorite (336 ± 5 Ma; U-Pb SHRIMP zircon age; Rodríguez et al., 2022), viii) the Reguengos de Monsaraz gabbro-diorite (337.4 ± 1.1 Ma and 338.6 ± 0.7 Ma; U-Pb ID-TIMS zircon age; Antunes et al., 2011), and ix) the Cabrela ignimbrite (335 ± 2 Ma; U-Pb SHRIMP zircon age; Pereira et al., 2020).

Field relationships and petrography

Vale de Maceiras gabbro and low-grade metamorphic host rocks

The Vale de Maceiras pluton, consisting of gabbroic and monzonitic rocks, crops out in an area of about 20 km^2 located between the Évora gneiss dome and the Badajoz-Cordoba shear zone (Fig. 1b, 2). The melanocratic rocks were emplaced into low-grade metasedimentary rocks variously assigned to the Silurian (Gonçalves et al., 1975), the Ordovician-Silurian (Oliveira et al., 1992) or the Silurian-Early Devonian (Piçarra, 2000) (Fig. 3a). The Vale de Maceiras pluton interior locally exposes E-W-trending, steeply dipping magmatic foliation (Fig. 4a,b). The host metasedimentary rocks contain a pervasive NW-SE-trending moderately to steeply dipping foliation (S_2) overprinted by an E-W-trending, steeply dipping crenulation cleavage (S_{2b}) (Fig. 4c,f). The foliation steeply dipping S_{2a} is commonly parallel to the compositional layering (bedding) and associated intrafolial folds (Fig. 4d,e).

Locally, in the hinge zones of microfolds, S_{2b} is oriented at an oblique angle to bedding planes and an earlier foliation is recognized (Fig. 5a). S_{2a} is defined by the alignment of elongated quartz, biotite (sometimes mica-fish) partially altered to chlorite, and opaque

minerals (Fig. 5a,b). Poikilitic idioblasts of andalusite also occur. They have straight or weak waving inclusion trails defining an internal undeformed or gently folded S_{2a} foliation. They are thus inter-tectonic between S_{2a} and S_{2b} or syn-tectonic relative to S_{2b} (Fig. 5c). Strong retrogression of andalusite porphyroblasts is observed. Quartz-rich veinlets concordant with foliation S_{2a} contain muscovite and chlorite. S_{2a} foliation is overprinted by variably spaced S_{2b} extensional crenulation cleavage (Fig. 5d). S_{2b} interpreted as an extensional crenulation cleavage, is parallel to the axial surfaces of folds developed in the whitish veinlets that are parallel to S_{2a}. S_{2b} spaced cleavage consisting of mica-rich cleavage domains and microlithons (Fig. 5d,e). Mica-rich cleavage domains become wider and isolate microlithons that contain folded foliation relics of S_{2a} oblique to the S_{2b}, locally preserved within andalusite porphyroblasts (Fig. 5e). In the contact aureole of the Vale de Maceiras gabbro, porphyroblasts of biotite have grown during syn-S_{2a} and syn-S_{2b} development and andalusite grew over S_{2a} and pre-existing S_{2b}. S_{2a} foliation and S_{2b} extensional crenulation cleavage developed during regional Variscan extensional D_2 deformation event whereas structures and foliations related to the Variscan contractional D_1 deformation event were not recognized. A later Variscan contractional D_3 deformation event produced folding, thrusting, and wrenching responsible for the steepening of the earlier structures and local crenulation of S_{2a} and S_{2b} fabrics. Interpretation of the porphyroblast growth vs. deformation phase relationships of the host low-grade metasedimentary rocks of the Vale de Maceiras pluton is illustrated in Figure 6a. The petrographic P-T path for the host rocks shows that D_2 planar fabrics (S_{2a} and S_{2b}) may have evolved under a L- to MT-LP Buchan-type metamorphic stage (M_2) as was previously described for the northeast hanging-wall block of the Evora gneiss dome (Dias da Silva et al., 2018) (Fig. 6c).

Campo Maior microdiorite and quartz-diorite, and high-grade metamorphic host rocks

The Campo Maior microdiorite and quartz-diorite pluton crops out in an area of 0.7 km^2 surrounded by migmatitic rocks of the Badajoz-Córdoba shear zone. The plutonic rocks have both irregular diffuse and sharp internal contacts (Fig. 7). The plutonic rocks also show sharp or diffuse contacts with migmatites, forming meter- to decameter-scale sigmoidal shape domains bounded by high-strain shear zones with high-temperature quartz-feldspathic mylonitic rocks. Migmatitic rocks include variably sized boudins of amphibolite. The mylonitic gneisses exhibit a pervasive steeply dipping foliation defined by the alternation of leucocratic bands of dynamically recrystallized feldspar and quartz, and melanocratic bands with oriented biotite, sillimanite, and garnet. Meter- to centimeter-scale boudins are elongated parallel to the gently plunging fold axes and stretching lineation of gneisses and migmatites. The Campo Maior quartz-diorite shows either sharp or irregular and diffuse contacts with migmatites. Contacts are parallel to, or crosscut the folded migmatitic foliation (Fig. 7c). These quartz-dioritic rocks show magmatic foliation defined by the orientation of biotite associated with schlieren (Fig. 7d). Orthomigmatites spatially associated with the quartz-diorite were also identified. These include mafic schollen and schlieren (Fig. 7a) containing biotite and amphibole surrounded by coarse-to medium-grained leucocratic and melanocratic mineral aggregates. Locally they are reworked along discrete NW-SE-trending steeply dipping high-strain shear bands (Fig. 7b). Porphyroblast-fabric relationships of the high-grade metamorphic country rocks of the Campo Maior plutonic rocks are illustrated in Figure 6b. Interpretation of the porphyroblast growth vs. deformation phase of these magmatic rocks, based on previous work on the Campo Maior migmatites described in the Portuguese sector of the Badajoz-Cordoba shear zone (Pereira et al., 2010 and references therein), indicates that S_{2a} and S_{2b} foliations may have developed under a HT-LP Buchan-type metamorphic stage (M_2), following an HT-HP metamorphic event (M_1) (Fig. 7c).

Analytical methods

Mineral chemistry

Five thin sections of samples from Campo Maior and Vale de Maceira were made and polished at the University of Évora (Portugal). Subsequently, they were analyzed to determine the major element composition of mineral phases using a JEOL JXA-8200 super probe at the University of Huelva (Spain). A combination of silicates and oxides was used for calibration. A beam of 5 μm diameter was used to analyze mineral phases to minimize Na migration. Results from microprobe analyses are listed in Table 1 (supplementary material).

Whole-rock geochemistry

Analyses of whole-rock geochemistry for major and trace elements have been performed by inductively coupled plasma mass spectrometry (ICP-MS) at the Geochronology and Isotope Geochemistry SGIker-Facility of the UPV/EHU (Spain) following procedures of García de Madinabeitia et al. (2008). Reagents were concentrated HF and HNO_3 Merck Pro-Analysi. Deionized water is obtained using a Millipore Elix device and refined to obtain a resistivity ≥ 18 MOhm-cm with a Barnstead EasyPure system. Indium and Bi solutions were used as internal standards, and multi-elemental solutions for the initial tuning and calibration of the spectrometer were prepared from PerkinElmer multi-element standard solutions for ICP, stabilized in HNO_3 2 to 6 %. The internal standard was added using an automatic online addition kit to prevent random errors. Weighing to 0.1 mg precision was done with an electronic balance GRAM SV 205-A. Calcination was performed in two steps, one hour each at ~500 and 1050 °C, in a muffle furnace to remove H_2O and compounds of C and S. The alkaline fusion of the samples was carried out using an automatic Claisse Fluxy 30 system over butane gas in Pt-Au (95-5) crucibles with lithium metaborate ($LiBO_2$) as flux and LiBr as the non-wetting agent. The melt was automatically poured into a polystyrene beaker containing 100 ml of HNO_3 and ~0.05 ml of HF and placed in a magnetic agitator. The

solution was gravimetrically diluted to a factor adequate for the analysis. Major and trace element concentrations were determined using a Thermo XSeries 2 ICP-MS equipped with a collision cell, an interphase specific for elevated total dissolved solids (Xt cones), a shielded torch, and a gas dilution system. A concentric nebulizer and quartz expansion chamber were employed. Whole-rock geochemistry results are listed in Table 2 (supplementary material).

U-Pb geochronology (ID-TIMS; SHRIMP)

Zircon separation was performed through traditional techniques using gravity separation. Selected crystals were hand-picked using a binocular lens.

Sample VMC-10 of the Vale de Maceiras gabbro and sample CAMP-1 of the Campo Maior microdiorite yielded few zircon grains. They were analyzed by ID-TIMS, starting with chemical abrasion (Mattinson, 2005). The grains were then cleaned and dissolved in HF (+HNO_3) at 195ºC for 5 days, after the addition of a ^{202}Pb-^{205}Pb-^{235}U spike. The purification of Pb and U follows Krogh (1973). Isotopic analyses were done with a combination of multi-collection on Faraday cups and peak jumping on a secondary electron multiplier of a MAT262 mass spectrometer at the University of Oslo. The data were corrected for blanks of ≤2pg Pb and 0.1 pg U. Other details of the procedure are described in Corfu (2004). Decay constants are from Jaffey et al. (1971) and ^{238}U/^{235}U = 137.88 was used.

The zircon grains of the Campo Maior quartz-diorite (sample CAMP-4) for SHRIMP analysis were cast on a 3.5cm diameter epoxy mount, together with zircon standards (TEMORA zircon, SL13 zircon, and GAL zircon), then polished and documented using SEM-CL, at the IBERSIMS (University of Granada, Spain). The mount was coated with gold (80 microns thick) and zircon analyzed by SHRIMP. Each selected spot was hit by the primary beam during 120s before analysis and then analyzed over 6 scans following the isotope peak

sequence $^{196}Zr_2O$, ^{204}Pb, 204.1 background, ^{206}Pb, ^{207}Pb, ^{208}Pb, ^{238}U, ^{248}ThO, ^{254}UO. Every peak of each scan was measured sequentially 10 times with the following total counts per scan: 2s for mass 196; 5 s for masses 238, 248, and 254; 15 s for masses 204, 206, and 208; and 20s for mass 207. The primary beam, composed of $^{16}O^{16}O^{2+}$, was set to an intensity of 4 to 5nA, using a 120-micron Kohler aperture, which generates 17 x 20-micron elliptical spots on the target. The secondary beam exit slit was set at 80 microns, achieving a resolution of about 5,000 at 1% peak height. All calibration procedures were performed on the standards included on the same mount. Mass calibration was performed on the GAL zircon (ca. 480 Ma, very high U, Th, and common lead content; Montero et al., 2008). Analytical sessions initially involved the measurement of SL13 zircon (Claoué-Long et al., 1995), which was used as a concentration standard (238 ppm U). TEMORA zircon (ca. 417 Ma, Black, et al., 2003), used as isotope ratios standard, was then measured every four unknowns. Data reduction was performed using the SHRIMPTOOLS software specifically developed by the IBERSIMS Laboratory. The intensity of each measured isotope was calculated in two steps using the software: first, the STATA letter value display algorithm was used to find outliers in the ten replicates measured at each peak during each scan, discarding them and averaging the rest once they had been normalized to SBM measurements; then, for each isotope, a robust regression of each scan average versus time, if measured, was performed. The result obtained for each isotope was calculated as the value at the mid-time of the analysis resulting from a robust regression line. Errors (95% confidence level) were calculated as the standard error of the linear prediction at the midpoint of the analysis. $^{206}Pb/^{238}U$ was calculated from the measured $^{206}Pb+/^{238}U+$ and UO^+/U^+ following the method described by Williams (1998). For high-U zircon grains (U > 2500 ppm) $^{206}Pb/^{238}U$ was corrected using the algorithm of Williams and Hergt (2000). Plotted and tabulated analytical uncertainties are 1σ precision estimates. Uncertainties in calculated mean ages are 95% confidence limits (tσ, where t is the

student's t multiplier) and, for mean $^{206}Pb/^{238}U$ ages, including the uncertainty in Pb/U calibration (0.3-0.5 %). Common Pb corrections assumed a model common Pb composition appropriate to the age of each spot (Cumming and Richards, 1975). U-Pb geochronology results are listed in Tables 3 and 4 (supplementary material).

Results

Geochemistry, petrography, and mineral chemistry

The sample from Vale de Maceiras (VMC-10) is classified as an Opx-bearing gabbro. The mineral assemblage is anorthitic plagioclase (with a mean composition of An_{68}), orthopyroxene (En_{68}), clinopyroxene (Wo_{42}, En_{42}, Fs_{15}), olivine (Fo_{64}), amphibole (Mg-Hbl), phlogopite (#Mg = 0.68; Table 1; supplementary material) and magnetite (Fig. 8a, b). Olivine has reaction rims replaced by orthopyroxene (Fig. 8c). Orthopyroxene is replaced by amphibole (Fig. 8c).

Samples from Campo Maior are classified as orthopyroxene-bearing microdiorite (CAMP-1) and quartz-diorite (CAMP-4). The former is characterized by a porphyritic texture with phenocrysts of orthopyroxene, plagioclase, clinopyroxene, biotite, and scarce amphibole (Fig. 8e) and a matrix composed of plagioclase, quartz, and poikilitic K-feldspar. The latter contains zoned plagioclase, amphibole (Mg-Hbl), biotite (#Mg = 0.54), K-feldspar, and quartz with cataclastic texture (Fig. 8f). The anorthite content in quartz-diorite is much lower than that of the gabbro (An_{31}; Table 1; supplementary material). Orthomigmatites (CAMP-2 and CAMP-3) have a quartz-dioritic composition with plagioclase, K-feldspar, biotite, amphibole, quartz, and opaques (Fig. 8g, h). Biotite alignment in these rocks defines a migmatitic foliation (Fig. 8h).

Igneous and metamorphic rocks from Campo Maior and Vale de Maceiras have a magnesian, metaluminous whole-rock geochemistry (Alumina Saturation Index-$Al_2O_3/[Na_2O+K_2O+(CaO-3.3*P_2O_5)]$ molar ratio < 1; Table 2; supplementary material). They plot into the subalkaline field (Fig. 9a) and may be classified as high-K calc-alkaline rocks (Fig. 9b). Geochemical discrimination diagrams used for distinguishing between calc-alkaline and sanukitoid (i.e. vaugneritic) series (Figs. 9c, d; Gómez-Frutos and Castro, 2022) include the cotectic lines and kernel density plots of sanukitoid data for comparison. These rocks indicate a sanukitoid affinity (Fig. 9c, d) instead of being related to the calc-alkaline cotectic as the igneous rocks from the Évora Massif were. Some of them (Opx-bearing gabbro and Opx-bearing microdiorite) show a compositional approximation to the mantle-derived melts, as the high Ni contents (about 100 ppm) and high #Mg for biotite and phlogopite (0.6-0.7). The sample composition plot in the Pearce's diagram shows that almost all samples are included in the field of volcanic arc granites (Fig. 9e).

Quartz-diorite and microdiorite have REE fractionated patterns, with LREE enrichment and flat HREE plot arrays (Fig. 10a). REE patterns for microdiorite and Qz-diorite differ in the extent of the negative Eu anomaly and in the HREE greater enrichment of the quartz-diorite (Fig. 10a) suggesting they differ in the extent of plagioclase fractionation. Orthomigmatites have upward concave patterns (Fig. 10b) indicating either amphibole fractionation or its occurrence as a peritectic phase in the partial melting process. Gabbro from Vale de Maceiras has low REE contents and a flat pattern for the HREE (Fig. 10c).

U-Pb zircon geochronology

Zircon grains extracted from the Vale de Maceiras gabbro (VMC-10) are stubby prismatic, euhedral, or irregular fragments. The crystals analyzed have U contents of 360-550 ppm and Th/U = 0.36-0.46. Four U-Pb ID-TIMS analyses are concordant. Three of them

overlap and define an average $^{206}Pb/^{238}U$ age of 337.9 ± 0.4 Ma (MSWD = 0.48; Fig. 11a). The remaining analysis is marginally younger at 336.8 Ma, likely due to minor Pb loss. The age of 337.9 ± 0.4 Ma is considered the best estimate for crystallization of the Vale de Maceiras gabbro.

The Campo Maior microdiorite (CAMP-1) has a variety of zircon types, including large sub-equant and partially euhedral crystals, some small, short prismatic crystals, and assorted fragments. The analyzed grains have U contents ranging from 235 to 1044 ppm and uniform Th/U (0.34-0.46). Three of the U-Pb ID-TIMS analyses overlap near the Concordia curve, defining an average $^{206}Pb/^{238}U$ age of 338.4 ± 1.0 Ma (MSWD = 1.3; Fig. 11b). The fourth analysis is 3% discordant and yields a $^{206}Pb/^{238}U$ age of 332.6 Ma, suggesting some Pb loss. The age of 338.4 ± 1.0 Ma is considered the best estimate for the crystallization age of the Campo Maior microdiorite.

The zircon grains from the Campo Maior quartz-diorite (sample CAMP-4) are prismatic euhedral (50-200 μm in diameter), equant to strongly elongated, and show concentric or banded zoning. A few composite grains have a variable-width concentric zoned rim surrounding unzoned and banded cores. A total of eleven U-Pb SHRIMP analyses yielded U and Th contents ranging from 132 to 1597 ppm and from 25 to 574 ppm, respectively, with Th/U = 0.11 - 0.54 (average of 0.29). In grain 10, the rim age is “older” than the core age, and thus both were excluded from the age calculation. A group of 9 grains yields $^{206}Pb/^{238}U$ ages between ca. 340-314 Ma (^{204}Pb-corrected) and a weighted mean age of 335 ± 4 Ma (MSWD = 0.78; Fig. 11c), which is considered the best estimate for the crystallization age of the Campo Maior quartz-diorite.

Discussion

Tectonic control on the emplacement of the Vale de Maceiras and Campo Maior high-K mafic-intermediate plutonic rocks

The Visean OMZ plutons were emplaced at different crustal levels at the same time the continental lithosphere was undergoing strong stretching associated with the development of major Variscan extensional D_2 shear zones and gneiss domes (Pereira et al., 2009; Dias da Silva et al., 2018). The Vale de Maceiras gabbro represents a syn-extensional intrusion emplaced at shallower crustal levels than the Campo Maior microdiorite and quartz-diorite (Fig. 12a). The Vale de Maceiras gabbro contact metamorphic minerals found in host low-grade metamorphic rocks grew coevally with kinematic indicators. The direction of the long axis of the biotite mica-fish is parallel to S_2 foliation (Fig. 12a$_1$). Andalusite overgrew S_{2a} that is preserved as microlithons bounded by the spaced S_{2b} extensional crenulation cleavage (Fig. 12a$_2$). This relationship suggests that andalusite is a syn-D_2 porphyroblast. The Vale de Maceiras pluton has intrusive contacts that are discordant but are parallel to S_{2a} and S_{2b}, and to a magmatic foliation with the same direction of S_{2b} extensional crenulation of the host rocks (Fig. 12a). These observations, as well as those observed for the Campo Maior microdiorite and quartz-diorite, suggest that these intrusions are syn-kinematic with the Variscan extensional D_2 deformation event (Fig. 12a).

The Campo Maior microdiorite, quartz-diorite, and orthomigmatites, with steeply dipping foliation, occur together in sigmoidal-shaped domains bounded by discrete NW-SE-trending high-strain D_2 shear zones with mylonitic gneisses. The variation from sharp though irregular to more diffuse intrusive contacts suggests that quartz-diorite and microdiorite were coeval. The foliation of the orthomigmatites and in these high-temperature D_2 shear zones is steeply dipping, as also with the foliation of the country rocks of the Vale de Maceiras pluton, because they are tilted as a result of the Variscan contractional D_3 deformation event (Fig.

12b,b_1). Field relationships suggest that the progressive and heterogeneous deformation of migmatites under high-temperature metamorphic conditions was at least partly coeval with the intrusion of the Campo Maior quartz-diorite and microdiorite (Fig. 12a,b_2). Syntectonic migmatites contain numerous concordant and discordant dykes of granitic rocks (leucosome), locally showing a nebulitic texture and including sigmoidal-shape biotite-amphibolite-rich schollen. Dioritic rocks show extensive magma mingling with granitic leucosome, suggesting they were contemporaneous with the crustal melting.

Timing of pluton emplacement and origin of the OMZ high-K mafic-intermediate magmatism

The Campo Maior and Vale de Maceiras plutonic rocks belong to the Visean OMZ magmatic province, which is unique for its larger volume of mafic-intermediate suites compared to other zones of Iberia (Castro, 2019). The new radiometric ages for the Vale de Maceiras gabbro (337.9 ± 0.4 Ma; U-Pb ID-TIMS zircon) and the Campo Maior microdiorite (338.4 ± 1 Ma; U-Pb ID-TIMS zircon) suggest that their crystallization was coeval, overlapping within error the crystallization age of Campo Maior quartz-diorite (335 ± 4 Ma; U-Pb SHRIMP zircon). These age relationships support the geochemical data and field observations for the coeval emplacement of these plutonic rocks. The Campo Maior and Vale de Maceiras plutonic rocks have the same age, within analytical uncertainty, as other Visean magmatic rocks (ca. 341-335 Ma) emplaced at different crustal levels in the OMZ (Fig. 13). At deep crustal levels, the Almansor granodioritic-tonalitic dykes and the Hospitais quartz-diorite pluton were emplaced in migmatites of the Évora gneiss dome footwall. At shallower crustal levels, the Arraiolos granite dikes (Pereira ert al., 2009) and the Divôr quartz-diorite pluton (Dias da Silva et al., 2018) are either concordant or discordant with the foliation of surrounding hanging-wall amphibolites, quartz-feldspathic gneisses, and mica schists. In the uppermost crust, the Visean Reguengos de Monsaraz pluton (Antunes et al., 2011), composed

of quartz-diorites and gabbro-diorites, cuts the S_2 foliation of the country-rock metabasites, quartzites, and slates. In the Cabrela Basin, Visean ignimbrite layers (Pereira et al., 2020) alternate with turbidite beds that contain olistoliths, indicating significant tectonic instability during sedimentation with large-scale mass movement (Pereira et al., 2012) (Fig. 13).

The Vale de Maceiras Opx-rich gabbro and the Campo Maior Opx-rich microdiorite are classified as high-K calc-alkaline and have geochemical affinity with sanukitoids (Fig. 9). They were considered to be of late Devonian age (Moita et al., 2005b; Lopes et al., 2005), but the new U-Pb zircon ages (ca. 338 Ma) indicate they are Visean. The data support the interpretation that the late Variscan potassic dykes of vaugneritic signature, previously described in the OMZ (Lains Amaral, 2017; Lains Amaral and Mata, 2018), were preceded by emplacement of early Carboniferous plutonic counterparts, such as Vale de Maceiras and Campo Maior high-K mafic-intermediate plutonic rocks. This enables us to extend to SW Iberia the distribution of Visean magmatic occurrences of sanukitoid/vaugnerite magmatism well-known in the European Variscan belt of Central Europe (von Raumer et al., 2014), and correlate it with vaugneritic enclaves, dated at ca 339 Ma, hosted in ca. 337 Ma granodiorites, in NW Iberia (Gutiérrez-Alonso et al., 2018).

The similar age and sanukitoid affinity of the Vale de Maceiras gabbro and the Campo Maior microdiorite and associated quartz-diorite are comparable with those of other plutonic rocks with variable calc-alkaline compositions of the Évora gneiss dome (Fig. 9). This suggests that magmas originated from different sources and in different tectonic environments and involved variable proportions of crustal and mantle components. Partial melting and recycling of old crustal sources (the Ediacaran Serie Negra metasedimentary rocks) might be exemplified by the peraluminous Arraiolos granites and Almansor monzonitic-monzogranitic diatexites (Pereira et al., 2009; Moita et al., 2009). Fractional crystallization from primitive

mafic magmas produced in the enriched mantle wedge above a subduction zone and mixing with variable proportions of crustal melts might be exemplified by the weakly peraluminous Almansor granodioritic-tonalitic dykes (Moita et al., 2009). The genesis of the coeval metaluminous Hospitais quartz-diorites might result from the differentiation of a mafic magma extracted from a mantle wedge enriched during subduction (Moita et al., 2015). The Visean metaluminous granitic rocks may have originated by mixing mafic magma derived from a depleted mantle source with a crustal melt presumably produced by the partial melting of the Cambrian calc-alkaline felsic igneous rocks of the Évora gneiss dome (Moita et al., 2015). Finally, the ca. 337-336 Ma Alto de São Bento weakly peraluminous tonalitic and metaluminous dioritic rocks may be readily associated with this scenario given their arc-like, calc-alkaline geochemical signatures (Rodríguez et al., 2022).

The Vale de Maceiras and Campo Maior mafic-intermediate rocks show geochemical features distinct from the calc-alkaline series. They have sanukitoid affinity probably inherited from a metasomatized mantle from which these rocks originate (Castro, 2020). In this regard, it may be noted that the coeval Beja-Acebuches mafic-ultramafic rocks dated at ca. 340-332 Ma (Azor et al., 2008) have a transitional composition between that of mid-ocean ridge and island arc basalts (Quesada et al., 1994; Castro et al., 1996), suggesting an origin from a depleted mantle source with different degrees of contamination by enriched melts.

Implications for regional tectonics

A rival interpretation presuming an intra-orogenic extensional event for the Carboniferous evolution in SW Iberia (Simancas et al., 2006; Pereira et al., 2009) has been proposed as an alternative to the tectonic models of sequential contractional deformation events (Ribeiro et al., 2007). The concurrent development of Early Carboniferous basins and felsic to mafic-intermediate volcanism (Santos et al., 1987, 1990; Armendáriz et al. 2008;

Pereira et al., 2020), together with the geochemical variations in plutonism (Moita et al., 2015; Cambeses et al. 2014; Jesús et al. 2016) and the onset of gneiss domes (Pereira et al., 2009; Dias da Silva et al., 2018), suggest the upwelling of the asthenosphere beneath the OMZ (Pereira et al., 2015). This large thermal anomaly would have propagated through the previously structured and thickened crust. Therefore, the low- to high-T and low-P metamorphism, associated with Variscan D_2 shearing, operated on different tectonostratigraphic units. Rodríguez et al. (2022) recently proposed a regional tectonic model of oblique ridge subduction and slab window development beneath the OMZ to explain the origin and geochemical changes in the Early Carboniferous arc magmatism in this region of Pangea. We suggest that the depleted mantle reservoir was probably emplaced beneath the OMZ through a slab window that formed during the subduction and migration of a spreading ridge, possibly a ridge from the Paleotethys Ocean. This slab window was the source of heat and magmas for the Visean Beja-Acebuches MORB and island arc basalts mafic-ultramafic rocks emplaced in a backarc setting (Quesada et al., 1994). Slab windows may cause magmatism in accretionary prism and forearc settings (Breitsprecher et al., 2003), but also influence magmatism further inboard, in the backarc setting (Cole et al., 2006). Visean quartz-diorite and associated gabbro-dioritic rocks have a calc-alkaline signature typical of magmas generated in a continental magmatic arc setting from subduction-related components coupled with crustal contamination (Moita et al., 2015). The subduction-related components (e.g. slab melts, fluids, or arc magmas) may either be stored in the subcontinental lithospheric mantle or contaminate the supra-subduction mantle wedge, or both (Gorring and Kay, 2001). The source of Visean sanukitoid magmas could have been peridotites from the enriched mantle wedge and partial melts of the subcontinental lithospheric mantle.

Peraluminous granitic rocks, discordant and concordant with the regional foliation of surrounding amphibolites, micaschists, gneisses, and migmatites (Moita et al., 2009; Dias da

Silva et al., 2018), preserve a large number of zircon xenocrysts. Those zircon grains survived through melting reactions giving important information on the heterogeneous ancient crustal source they are derived from. Visean peraluminous granitic rocks are most likely the result of partial melting of Ediacaran and Cambrian metasedimentary and metaigneous rocks (Pereira et al., 2009). Therefore, the origin of crustal-derived magma and melting mechanism may be related to heat transfer from rising asthenosphere and mantle magmas. High heat flow through the dynamics of the subduction system, including the development of a slab window and syn-kinematic high-temperature metamorphism, may have induced partial melting of the i) oceanic lithosphere; ii) supra-subduction mantle wedge; iii) sub-continental mantle; iv) Carboniferous arc roots, and v) host metasedimentary and metaigneous rocks, to account for the great compositional variety the OMZ plutonic rocks.

Conclusions

Field and U-Pb zircon geochronology evidence suggest the OMZ high-K mafic-intermediate magmas are spatially related. The syn-tectonic nature of the Vale de Maceiras pluton is attested by (i) the intrusive contacts discordant but also parallel to S_{2a} foliation and S_{2b} extensional crenulation cleavage, (ii) the magmatic foliation parallel to S_{2b}, and (iii) the contact metamorphism minerals (biotite and andalusite) that grew at the same time as S_{2a} and S_{2b}, as the result of the progressive Variscan extensional D_2 deformation event. The Vale de Maceiras pluton was dated at 337.9 ± 0.4 Ma (ID-TIMS), and thus the regional foliation is reinterpreted as S_2. The Campo Maior microdiorite, quartz-diorite, and orthomigmatites are spatially linked to high-temperature mylonitic gneisses formed in D_2 high-strain shear zones. Field relationships suggest that the progressive deformation of migmatites was partly coeval with the intrusion of the Campo Maior quartz-diorite and microdiorite. The Campo Maior microdiorite and quartz-diorite were dated at 338.4 ± 1 Ma (ID-TIMS) and 335 ± 4 Ma

(SHRIMP), respectively. The ages coincide with the previously established age of metamorphism. The Vale de Maceiras gabbro and the Campo Maior microdiorite and quartz-diorite are coeval syn-tectonic intrusions emplaced at different crustal levels during Visean extensional tectonics. The Vale de Maceiras and Campo Maior mafic-intermediate rocks have geochemical features distinct from the calc-alkaline series, showing affinity with sanukitoids. The new data have improved the existing knowledge about the geochemical variability of the Visean OMZ plutonic rocks (ca. 349-335 Ma) referred to in previous studies, from tholeiitic to calc-alkaline and sanukitoid affinity, which may be explained by the partial melting of mantle domains contaminated by crustal material during subduction.

Acknowledgments

This study is a tribute to Prof. Maarten de Wit and to Prof. Ana Neiva who contributed decisively to advancing the knowledge of the Paleozoic plutonic rocks of Iberia. This research was funded by the Spanish Agency of Science and Technology Grant N° PGC2018-096534-B-I00 (Project IBERCRUST). M.F.P. acknowledges financial support from the Portuguese Foundation for Science and Technology project FCT/UIDB/04683/2020- ICT. C.R. acknowledges her postdoc contract funded by FEDER/Junta de Andalucía-Consejería de Economía y Conocimiento (DOC-01689). I.D.S. acknowledges financial support from the FCT and I.P./MCTES (FCT/UID/GEO/50019/2019-IDL and FCT/UIDB/ 50019/2020-IDL), his national science contract in the FCUL funded by FCT “Estímulo ao Emprego Científico-Norma Transitória”., and project grant PID2020-117332GB-C21 (Spanish Agency of Science and Technology). This work is a contribution to IDL Research Group 3 (Solid Earth Dynamics, Hazards and Resources). IBERSIMS publication number 101. Careful reviews by J. Brendan Murphy (Coordinating Editor) and referees contributed to improving the manuscript.

References

Abati, J., Arenas, R., Díez Fernández, R., Albert, R., Gerdes, A., 2018. Combined zircon U-Pb and Lu-Hf isotopes study of magmatism and high-P metamorphism of the basal allochthonous units in the SW Iberian Massif (Ossa-Morena complex). *Lithos* 322, 20-37.

Antunes, A., Santos, J.F., Azevedo, M.R., Corfu, F., 2011. New U–Pb zircon age constraints for the emplacement of the Reguengos de Monsaraz Massif (Ossa Morena Zone). *Seventh Hutton symposium on granites and related rocks*- abstracts book, Ávila, 9–10.

Armendáriz, M., López-Guijarro, R., Quesada, C., Pin, C., Bellido, F., 2008. Genesis and evolution of a syn-orogenic basin in transpression: Insights from petrography, geochemistry and Sm-Nd systematics in the Variscan Pedroches basin (Mississippian, SW Iberia). *Tectonophysics*, 461, 395-413.

Azor, A., Lodeiro, F.G., Simancas, J.F., 1994. Tectonic evolution of the boundary between the central Iberian and Ossa-Morena zones (Variscan belt, Southwest Spain). *Tectonics* 13 (1), 45-61.

Azor, A., Rubatto, D., Simancas, J.F., González Lodeiro, F., Martínez Poyatos, D., Martín Parra, L.M., Matas, J., 2008. Rheic Ocean ophiolitic remnants in southern Iberia questioned by SHRIMP U-Pb zircon ages on the Beja-Acebuches amphibolites. *Tectonics*, 27, TC5006.

Black, L.P., Kamo, S.L., Williams, I.S., Mundil, R., Davis, D.W., Korsch, R.J., Foudoulis, C., 2003. The application of SHRIMP to Phanerozoic geochronology, a critical appraisal of four zircon standards. *Chemical Geology*, 200, 171-188.

Breitsprecher, K., Thorkelson, D.J., Groome, W.G., Dostal, J., 2003. Geochemical confirmation of the Kula-Farallon slab window beneath the Pacific Northwest in Eocene time. *Geology*, 31, 351-354.

Burg, J.P., Iglesias, M., Laurent, P., Matte, P., Ribeiro, A., 1981. Variscan intracontinental deformation: the Coimbra-Cordoba shear zone (SW Iberian Peninsula). *Tectonophysics* 78 (1-4), 161-177.

Cambeses, A., Scarrow, J.H., Montero, P., Molina, J.F., Moreno, J.A., 2015. SHRIMP U-Pb zircon dating of the Valencia del Ventoso plutonic complex, Ossa-Morena Zone, SW Iberia: Early Carboniferous intra-orogenic extension-related 'calc-alkaline' magmatism. *Gondwana Research*, 28, 735-756.

Castro, A., 2019. Variscan Magmatism. 13.3 An Overview on the Petrogenesis of the Large Batholiths and the Mantle-Related, Basic and Intermediate Rocks. In: Quesada, C., Oliveira, J.T. (eds*), The Geology of Iberia: A Geodynamic Approach*, Volume 2: The Variscan Cycle, Regional Geology Reviews, Springer-Verlag, 514-521.

Castro, A., 2020. The dual origin of I-type granites: the contribution from experiments. *Geological Society, London, Special Publications* 491, 101-145.

Castro, A., 2021. A non-basaltic experimental cotectic array for calc-alkaline batholiths. *Lithos*, v. 382-383, p. 105929.

Castro, A., Fernández, C., de la Rosa, J.D., Moreno-Ventas, I., El Hmidi, H., El Biad, M., Bergamin, J.F., Sánchez, N., 1996. Triple-junction migration during Paleozoic Plate convergence: The Aracena metamorphic belt, Hercynian massif, Spain, *Geologische Rundschau*, 85, 108-185.

Claoué-Long, J.C., Compston, W., Roberts, J., Fanning, C.M., 1995. Two Carboniferous ages: a comparison of SHRIMP zircon dating with conventional zircon ages and $^{40}Ar/^{39}Ar$ analysis. In: Berggren, W. A., Kent, D. V., Aubry, M. P., Hardenbol, J., (eds.). Geochronology Time Scales and Global Stratigraphic Correlation. *Society for Sedimentary Geology (SEPM*), Special Publication No. 4, 3-21.

Cole, R.B., Nelson, S.W., Layer, P.W., Oswald, P.J., 2006. Eocene volcanism above a depleted mantle slab window in southern Alaska. *GSA Bulletin*, 118, 1/2, 140-158.

Corfu, F. 2004. U-Pb age, setting, and tectonic significance of the anorthosite-mangerite charnockite-granite-suite, Lofoten-Vesterålen, Norway. *Journal of Petrology* 45, 1799-1819.

Cumming, G.L., Richards, J.R., 1975. Ore lead isotope ratios in a continuously changing earth. *Earth and Planetary Science Letters*, 28, 155-171.

Dallmayer, R.D., Martínez Garcia, E., 1990. *Pre-Mesozoic Geology of Iberia*. Springer-Verlag, 416p.

Dias da Silva, Í., Pereira, M.F., Silva, J.B., Gama, C., 2018. Time-space distribution of silicic plutonism in a gneiss dome of the Iberian Variscan Belt: The Évora Massif (Ossa-Morena Zone, Portugal). *Tectonophysics*, 747-748, 298-317.

Díez Fernández, R., Arenas, R., Pereira, M.F., Sánchez Martínez, S., Albert, R., Martín Parra, L.M., Rubio Pascual, F.J., Matas, J., 2016. Tectonic evolution of Variscan Iberia: Gondwana-Laurussia collision revisited. *Earth-Science Reviews*, 162, 269–292.

Díez Fernández, R., Pereira, M.F., Foster, D.A., 2015. Peralkaline and alkaline magmatism of the Ossa-Morena zone (SW Iberia): age, source, and implications for the Paleozoic evolution of Gondwanan lithosphere. *Lithosphere*, 7, 73-92.

Díez-Fernández, R.D., Fuenlabrada, J.M., Chichorro, M., Pereira, M.F., Sánchez-Martínez, S., Silva, J.B., Arenas, R., 2017. Geochemistry and tectonostratigraphy of the basal allochthonous units of SW Iberia (Évora Massif, Portugal): Keys to the reconstruction of pre-Pangean paleogeography in southern Europe: *Lithos*, 268–271, 285–301.

Eguiluz, L., Ibarguchi, J.G., Abalos, B., Apraiz, A., 2000. Superposed Hercynian and Cadomian orogenic cycles in the Ossa-Morena zone and related areas of the Iberian massif. *GSA Bulletin* 112 (9), 1398-1413.

García de Madinabeitia, S., Sánchez Lorda, M.E., Gil Ibarguchi, J.I., 2008. Simultaneous determination of major to ultratrace elements in geological samples by fusion-dissolution and inductively coupled plasma mass spectrometry techniques. *Analytica Chimica Acta*, 625, 2, 117-130.

Gómez-Frutos, D., and Castro, A., 2022, Sanukitoid crystallization relations at 1.0 and 0.3 GPa. *Lithos*, v. 414-415, p. 106632.

Gonçalves, F., Ladeira, F.L., Joaquim, A.N. 1975. *Notícia explicativa da Carta Geológica de Portugal, 1:50.000, Folha 32D (Sousel)*. Serviços Geológicos de Portugal, Lisboa.

Gorring, M.L., Kay, S.M., 2001. Mantle processes and sources of Neogene slab window magmas from Southern Patagonia, Argentina. *Journal of Petrology* 42, 1067-1094.

Gutiérrez-Marco, J.C., Piçarra, J.M., Meireles, C.A., Cózar, P., García-Bellido, D.C., Pereira, Z., Vaz, N., Pereira, S., Lopes, G., Oliveira, J.T., Quesada, C., Zamora, S., Esteve, J., Colmenar, J., Bernárdez, E., Coronado, I., Lorenzo, S., Sá, A.A., Dias da Silva, Í., González-Clavijo, E., Díez-Montes, A., Gómez-Barreiro, J., 2019. Early Ordovician–Devonian Passive Margin 3 Stage in the Gondwanan Units of the Iberian Massif. In: Quesada, C., Oliveira, J.T. (eds*), The Geology of Iberia: A Geodynamic Approach*, Volume 2: The Variscan Cycle, Regional Geology Reviews , Springer-Verlag, 75-98.

Gutiérrez-Alonso, G., Fernández-Suárez, J., López-Carmona, A., and Gärtner, A., 2018, Exhuming a cold case: The early granodiorites of the northwest Iberian Variscan belt- A Visean magmatic flare-up? *Lithosphere*, 10, no. 2, 194-216.

Irvine, T.N., and Baragar, W.R.A., 1971, A Guide to the Chemical Classification of the Common Volcanic Rocks. *Canadian Journal of Earth Sciences*, v. 8, no. 5, p. 523-548.

Jaffey, A.H., Flynn, K.F., Glendenin, L.E., Bentley, W.C., Essling, A.M., 1971. Precision measurement of half-lives and specific activities of ^{235}U and ^{238}U. *Physical Review*, Section C, Nuclear Physics 4, 1889 1906.

Jesus, A.P., Mateus, A., Munhá, J.M., Tassinari, C.G., Bento dos Santos, T.M., Benoit, M., 2016. Evidence for underplating in the genesis of the Variscan synorogenic Beja Layered Gabbroic Sequence (Portugal) and related mesocratic rocks. *Tectonophysics*, 683, 148-171.

Krogh, T.E. 1973. A low contamination method for hydrothermal decomposition and extraction of U and Pb for isotopic age determinations. *Geochimica et Cosmochimica Acta* 37, 485- 494.

Lains Amaral, A., Moita, P., Lopes, J.M.C., Mata, J., 2019. Variscan Magmatism. 13.2.4 Late-Devonian Shoshonitic Magmatism at the Ossa-Morena Zone. In: Quesada, C., Oliveira, J.T. (eds*), The Geology of Iberia: A Geodynamic Approach*, Volume 2: The Variscan Cycle, Regional Geology Reviews, Springer-Verlag, 505-507.

Lains Amaral, J. Mata, J., 2018. On the late-Variscan occurrence of high-K dykes at the Ossa-Morena Zone. *XIV Congresso de Geoquímica dos Países de Língua Portuguesa e XIX Semana de Geoquímica*. Vila Real, Livro de Atas, 52-56.

Lains Amaral, J., 2017, Petrologia e Geoquímica dos maciços shoshoníticos de Veiros e Vale de Maceira (Zona de Ossa-Morena): implicações geodinâmicas. M.Sc. thesis, Universidade de Lisboa.

Lima, S.M., Corfu, F., Neiva, A.M.R., Ramos, M.F., 2012. Dissecting complex magmatic processes: an in-depth U-Pb study of the Pavia Pluton, Ossa-Morena Zone, Portugal. *Journal of Petrology* 53, 1887-1911.

Lopes, J.M.C., Munhá, J., Tassinari, C., Pin, C., 2005. Petrologia e geocronologia, Sm-Nd, do maciço de Campo Maior, Alentejo, Portugal central. *Comunicações Geológicas* 92, 5-30.

Lopes, J.M.C., 2004. Petrologia e Geoquímica de Complexos Plutónicos do NE Alentejano (Z.O.M.), Portugal central - Província Alcalina e Maciço de Campo Maior. *Unpublished Ph.D. thesis*, Universidade de Évora, 505 pp.

Martínez Catalán, J.R., Schulmann, K., Ghienne, J.-F. 2021. The Mid-Variscan Allochthon: Keys from correlation, partial retrodeformation and plate-tectonic reconstruction

to unlock the geometry of a non-cylindrical belt. *Earth-Science Reviews*, 220, 103700, https://doi.org/https://doi.org/10.1016/j.earscirev.2021.103700.

Martínez-Catalán, J.R., Arenas, R., Diaz Garcıa, F., Gomez-Barreiro, J., Gonzalez Cuadra, P., Abati, J., Castineiras, P., Fernandez-Suarez, J., Sanchez Martınez, S., Andonaegui, P., Gonzalez Clavijo, E., Dıez Montes, A., Rubio Pascual, F.J., Valle Aguado, B., 2007. Space and Time in the Tectonic Evolution of the Northwestern Iberian Massif. Implications for the Comprehension of the Variscan Belt. In: Hatcher Jr., R.D., Carlson, M.P., McBride, J.H., Martınez-Catalan, J.R. (Eds.), 4-D Framework of Continental Crust. *GSA Memoir*, Boulder, Colorado, 403-423.

Matte, Ph., 1991. Accretionary history and crustal evolution of the Variscan belt in Western Europe. *Tectonophysics* 196, 309–337.

Mattinson, J.M. 2005. Zircon U-Pb chemical abrasion ("CA-TIMS") method: Combined annealing and multi-step partial dissolution analysis for improved precision and accuracy of zircon ages. *Chemical Geology* 220, 47–66, doi.org/10.1016/j.chemgeo.2005.03.011

Moita, P., Munhá, J., Fonseca, P., Tassinari, C., Araújo, A., Palácios, T., 2005b. Dating orogenic events in Ossa-Morena Zone. *Actas do XIV Semana de Geoquímica/VIII Congresso de Geoquímica dos Países de Língua Portuguesa.* Universidade de Aveiro, 459-462.

Moita, P., Munhá, J., Fonseca, P.E., Pedro, J., Tassinari, C.C.G., Araújo, A., Palacios, T., 2005a. Phase equilibria and geochronology of Ossa-Morena eclogites. XIV Semana de Geoquímica, Actas do XIV Semana de Geoquímica/VIII Congresso de Geoquímica dos Países de Língua Portuguesa. Universidade de Aveiro, 463–466.

Moita, P., Santos, J.F,; Pereira, M.F., Costa, M.M., Corfu, F., 2015. The quartz-dioritic Hospitais intrusion (SW Iberian Massif) and its mafic micro-granular enclaves- Evidence for mineral clustering. *Lithos*, 224–225, 78-100.

Moita, P., Santos, J.F., Pereira, M.F., 2009. Layered granitoids: Interaction between continental crust recycling processes and mantle-derived magmatism: Examples from the Évora Massif (Ossa–Morena Zone, southwest Iberia, Portugal). *Lithos*, 111, 125-141.

Montero, P., Bea, F., Corretgé, L.G., Floor, P., Whitehouse, M.J., 2008. U-Pb ion microprobe dating and Sr-Nd isotope geology of the Galiñeiro Igneous Complex. A model for the peraluminous/peralkaline duality of the Cambro-Ordovician magmatism of Iberia. *Lithos*, 107, 227-238.

Montero, P., Salman, K., Bea, F., Azor, A., Exposito, I., González-Lodeiro, F., Martinez Poyatos, D.J., Simancas, J.F.., 2000. New data on the geochronology of the Ossa Morena Zone, Iberian Massif. *Basement Tectonics* 15, 136–138.

Murphy, J.B., Quesada, C., Gutiérrez-Alonso, G., Johnston, S.T., Weil, A., 2016. Reconciling competing models for the tectono-stratigraphic zonation of the Variscan orogen in Western Europe. *Tectonophysics* 681, 209–219.

Nakamura, N., 1974, Determination of REE, Ba, Fe, Mg, Na and K in carbonaceous and ordinary chondrites. *Geochimica et Cosmochimica Acta*, v. 38, p. 757-775.

Oliveira, J.T., Pereira, E., Ramalho, M.; Antunes, M.T., Monteiro, J.H., 1992. *Carta Geológica de Portugal*, scale 1/500.000. Serviços Geológicos de Portugal.

Passchier, C.W., Trouw, R.A.J., 2005. *Microtectonics*, 2nd ed. Springer-Verlag, Berlin.

Pearce, J. A., Harris, N., Tindle, A. G., 1984, Trace element discrimination diagrams for the tectonic interpretation of granitic rocks, *Journal of Petrology*, 25, 956-983.

Peccerillo, A., and Taylor, S. R., 1976, Geochemistry of Eocene calc-alkaline volcanic rocks from the Kastamonu area, Northern Turkey. *Contributions to Mineralogy and Petrology*, v. 58, no. 1, p. 63-81.

Pereira, M.F., Fuenlabrada, J.M., Rodríguez, C., Castro, A., 2022. Changing Carboniferous Arc Magmatism in the Ossa-Morena Zone (Southwest Iberia): Implications for the Variscan Belt. *Minerals* 12, 597.

Pereira, M.F., Gama, C., Dias da Silva, Í., Silva, J.B., Hoffmann, M., Linnemann, U., Gärtner, A., 2020. Chronostratigraphic framework and provenance of the Ossa-Morena Zone Carboniferous basins (southwest Iberia). *Solid Earth*, 11, no. 4, 1291-1312.

Pereira, M.F., Gutiérrez-Alonso, G., Murphy, J.B., Drost, K., Gama, C., Silva, J.B., 2017. Birth and demise of the Rheic Ocean magmatic arc(s): Combined U-Pb and Hf isotope analyses in detrital zircon from SW Iberia siliciclastic strata. *Lithos*, 278-281, 383-399.

Pereira, M.F., Chichorro, M., Moita, P., Santos, J.F., Solá, A.M.R., Williams, I.S., Silva, J.B., Armstrong, R.A., 2015. The multistage crystallization of zircon in calc-alkaline granitoids: U-Pb age constraints on the timing of Variscan tectonic activity in SW Iberia. *International Journal of Earth Sciences* 104, 5, 1167-1183.

Pereira, M.F., Chichorro, M., Silva, J., Ordóñez-Casado, B., Lee, J., Williams, I., 2012. Early Carboniferous wrenching, exhumation of high-grade metamorphic rocks, and basin instability in SW Iberia; constraints derived from structural geology and U–Pb and ^{40}Ar-^{39}Ar geochronology. *Tectonophysics*, 558-559, 28-44.

Pereira, M.F., Apraiz, A., Chichorro, M., Silva, J.B., Armstrong, R.A., 2010. Exhumation of high-pressure rocks in northern Gondwana during the Early Carboniferous (Coimbra-Cordoba shear zone, SW Iberian Massif): Tectonothermal analysis and U-Th-Pb SHRIMP in-situ zircon geochronology. *Gondwana Research* 17 (2-3), 440-460.

Pereira, M.F., Chichorro, M., Williams, I.S., Silva, J.B., Fernandez, C., Diaz-Azpiroz, M., Apraiz, A., Castro, A., 2009. Variscan intra-orogenic extensional tectonics in the Ossa-Morena Zone (Évora-Aracena-Lora del Rio metamorphic belt, SW Iberian Massif): SHRIMP zircon U-Th-Pb geochronology. In: Murphy, J.B., Keppie, J.D., Hynes, A.J. (eds.), *Ancient Orogens and Modern Analogues*, GSA-SP, 327, 215-237.

Pereira, M.F., Chichorro, M., Williams, I.S., Silva, J.B., 2008a. Zircon U-Pb geochronology of paragneisses and biotite granites from the SW Iberia Massif. (Portugal): evidence for a paleogeographic link between the Ossa-Morena Ediacaran basins and the West African craton. In: Ennih, N., Liégeois, J.P. (eds.), *The Boundaries of the West African Craton*. GSA-SP 297, 385-408.

Pereira, M.F., Apraiz, A., Silva, J.B., Chichorro, M., 2008b. Tectonothermal analysis of high-temperature mylonitization in the Coimbra–Córdoba shear zone (SW Iberian Massif, Ouguela tectonic unit, Portugal): evidence of intra-continental transcurrent transport during the amalgamation of Pangea. *Tectonophysics* 461 (1-4), 378-39.

Pérez-Cáceres, I., Martínez Poyatos, D., Simancas, J.F., Azor, A., 2015. The elusive nature of the Rheic Ocean suture in SW Iberia, *Tectonics*, 34, 2429-2450.

Piçarra, J.M. 2000. *Estudo estratigráfico do sector Estremoz-Barrancos, Zona de Ossa Morena, Portugal.* Unpublished Ph.D. thesis, Universidade de Évora.

Pin, Ch., Rodríguez, J., 2009. Comment on "Rheic Ocean ophiolitic remnants in southern Iberia questioned by SHRIMP U-Pb zircon ages on the Beja-Acebuches amphibolites" by A. Azor et al., *Tectonics*, https://doi.org/10.1029/2009TC002495

Pin, Ch., Fonseca, P.E., Paquette, J.L., Castro, P., Matte, Ph., 2008. The ca. 350 Ma Beja igneous complex: a record of transcurrent slab break-off in the southern Iberia Variscan Belt? *Tectonophysics*, 461, 356-377.

Pinto Coelho, A. V., Gonçalves, F., 1972. Nota previa sobre o provável Precambrico mais antigo do Alto Alentejo. Serie de afinidade charnoquitica de Campo Maior. *Boletim do Museu e Laboratório de Mineralogia e Geologia. da Faculdade de Ciencias de Lisboa* 13, 59-81.

Pinto Coelho, A.V., Gonçalves, F., Torquato, J.R., 1974. Rochas hipersténicas do Alto-Alentejo. *Boletín Geológico y Minero* 15, 601-603.

Quesada, C., Fonseca, P.E., Munha, J., Oliveira, J.T., Ribeiro, A., 1994. The Beja-Acebuches Ophiolite (Southern Iberia Variscan fold belt): geological characterization and significance. *Boletin Geológico y Minero* 105, 3-49.

Quesada, C., Robardet, M., Gabaldon, V., 1990. Ossa-Morena Zone. Stratigraphy. Synorogenic phase (Upper Devonian- Carboniferous-Lower Permian), in: Dallmeyer, R.D., Martínez García, E. (eds*)*, *Pre-Mesozoic Geology of Iberia*, edited by Springer-Verlag, Berlin-Heidelberg 273–279.

Ribeiro, M.L., Castro, A., Almeida, A., González Menéndez, L., Jesus, A., Lains, J. A., Lopes, J.C. Martins, H.C.B., Mata, J., Mateus, A., Moita, P., Neiva, A.M.R., Ribeiro, M.A., Santos, J.F., and Solá, A.R., 2019. Variscan Magmatism. In: Quesada, C., Oliveira, J.T. (eds*)*,

The Geology of Iberia: A Geodynamic Approach, Volume 2: The Variscan Cycle, Regional Geology Reviews, Springer-Verlag, 497-526.

Ribeiro, A., Munhá, J., Fonseca, P.E., Araújo, A., Pedro, J.C., Mateus, A., Tassinari, C., Machado, G., Jesus, A., 2010. Variscan ophiolite belts in the Ossa-Morena Zone (Southwest Iberia): geological characterization and geodynamic significance. *Gondwana Research* 17, 408-421.

Ribeiro, A., Munhá, J., Dias, R., Mateus, A., Pereira, E., Ribeiro, L., Fonseca, P., Araújo, A., Oliveira, T., Romão, J., Chaminé, H., Coke, C., Pedro, J., 2007. Geodynamic evolution of the SW Europe Variscides. *Tectonics***,** 26, TC6009.

Ribeiro, A., Quesada, C., Dallmeyer, R.D., 1990. Geodynamic evolution of the Iberian Massif. In: Dallmayer, R.D., Martínez Garcia, E., *Pre-Mesozoic Geology of Iberia*. Springer-Verlag, 399-409.

Robardet M., Gutiérrez-Marco J.C., 2004. The Ordovician, Silurian and Devonian sedimentary rocks of the Ossa Morena Zone (SW Iberian Peninsula, Spain), *Journal of Iberian Geology* 30, 73-92.

Rodriguez, C., Pereira, M.F., Castro, A., Gutiérrez-Alonso, G., Fernández, C. 2022. Variscan intracrustal recycling by melting of Carboniferous arc-like igneous protoliths (Évora Massif, Iberian Variscan belt). *GSA Bulletin*, 134 (5-6): 1549–1570.

Romeo, I., Lunar, R., Capote, R., Quesada, C., Dunning, G.R., Pina, R., Ortega, L., 2006. U-Pb age constraints on Variscan magmatism and Ni-Cu-PGE metallogeny in the Ossa-Morena Zone (SW Iberia). *Journal of the Geological Society*, 163, 837-846.

Rosas, F.M., Marques, F.O., Ballèvre, M., Tassinari, C., 2008. Geodynamic evolution of the SW Variscides: Orogenic collapse shown by new tectonometamorphic and isotopic data from western Ossa-Morena Zone, SW Iberia. *Tectonics*, vol. 27, TC6008, doi:10.1029/2008TC002333

Rubenach, M.J., Bell, T.H., 1988. Microstructural controls and the role of graphite in matrix/porphyroblast exchange during synkinematic andalusite growth in a granitoid aureole. *Journal of Metamorphic Geology* 6, 651-666.

Sánchez Carretero, R., Eguíluz, L., Pascual, E., Carrecedo, M., 1990. Ossa-Morena Zone. Igneous rocks, in: Dallmeyer, R.D., Martínez García, E. (eds), *Pre-Mesozoic Geology of Iberia*, Springer-Verlag, Berlin-Heidelberg 292-313.

Sánchez-García, T., Pereira, M.F., Bellido, F., Chichorro, M., Silva, J.B., Valverde-Vaquero, P., Pin, Ch., Solá, A.R., 2013. Early Cambrian granitoids of the Ossa-Morena Zone (SW Iberia) in the transition from a convergent setting to intra-continental rifting in the Northern margin of Gondwana. *International Journal of Earth Sciences*, 103, 1203-1218.

Sánchez-García, T., Bellido, F., Pereira, M.F., Chichorro, M., Quesada, C., Pin, C., Silva, J.B., 2010. Rift related volcanism predating the birth of the Rheic Ocean (Ossa-Morena Zone, SW Iberia). *Gondwana Research*, 17(2–4), 392–407.

Sánchez-Lorda M.E., Ábalos B., García de Madinabeitia S., Eguíluz L., Gil Ibarguchi J.I., Paquette J.L., 2016. Radiometric discrimination of pre-Variscan amphibolites in the Ediacaran Serie Negra (Ossa-Morena Zone, SW Iberia). *Tectonophysics* 681, 31-46.

Santos, J., Mata, J., Gonçalves, F., Munhá, J., 1987. Contribuição para o conhecimento Geológico-Petrológico da Região de Santa Susana: O Complexo Vulcano-sedimentar da Toca da Moura. *Comunicações dos Serviços Geológicos de Portugal*, 73 (1-2), 29-48.

Santos, J.F., Andrade, A.S., Munhá, J., 1990. Magmatismo orogénico Varisco no limite meridional da Zona de Ossa-Morena. *Comunicações dos Serviços Geológicos de Portugal* 76, 91-124.

Simancas, J.F., Azor, A., Martínez-Poyatos, D., Tahiri, A., El Hadi, H., González-Lodeiro, F., Pérz Estaún, A., Carbonell, R., 2009. Tectonic relationships of Southwest Iberia with the allochthons of Northwest Iberia and the Moroccan Variscides. *Comptes Rendus Geoscience* 341 (2-3), 103-113.

Simancas, J.F., Carbonell, R., González Lodeiro, F., Pérez Estaún, A., Juhlin, C., Ayarza, P., Kashubin, A., Azor, A., Martínez Poyatos, D., Sáez, R., Almodóvar, G.R., Pascual, E., Flecha, I., Martí, D., 2006. Transpressional collision tectonics and mantle plume dynamics: the Variscides of southwestern Iberia. In: Gee, D.G., Stephenson, R.A. (eds), European Lithosphere Dynamics. Geological Society, London, Memoirs 32, 345-354.

Simancas, J.F., A., Martínez Poyatos, D., Expósito, I., Azor, A., González Lodeiro, F., 2001. Th estructure of a major suture zone in the SW Iberian Massif: the Ossa-Morena/Central Iberian contact. *Tectonophysics* 332, 295-308.

Solís-Alulima, B., López-Carmona, A., Abati, J., 2020. Ordovician metamorphism and magmatism preserved in the Ossa Morena Complex: SHRIMP geochronology, geochemistry and Sr-Nd isotopic signatures of the Sierra Albarrana Domain (SW Iberian Massif). *Lithos* 374-375.

Spear, F.S., 1995. Metamorphic Phase Equilibria and Pressure-Temperature-Time Paths, 2nd ed. Mineralogical Society of America, Chelsea.

von Raumer, J.F., Finger, F-, Veselá, P., Stampfli, G.M., 2014. Durbachites-Vaugnerites- a geodynamic marker in the central European Variscan orogen. *Terra Nova*, 26, 85-95.

Wagner, R.H., 2004. The Iberian Massif: a Carboniferous assembly. *Journal of Iberian Geology*, 30, 93-108.

Whitney, D. L., and Evans, B. W., 2010, Abbreviations for names of rock-forming minerals: *American Mineralogist*, v. 95, no. 1, p. 185-187.

Williams, I.S., 1998. U-Th-Pb Geochronology by Ion Microprobe. In: McKibben, M. A., Shanks III, W. C., Ridley, W. I. (eds.). Applications of microanalytical techniques to understanding mineralizing processes. *Reviews in Economic Geology*, 7, 1-35.

Williams, I.S., Hergt, J.M., 2000. U-Pb dating of Tasmanian dolerites: a cautionary tale of SHRIMP analysis of high-U zircon. In: J.D. Woodhead, J.M. Hergt, W.P. Noble (eds.). *Beyond 2000: new frontiers in isotope science*. Lorne, Abstracts and Proceedings, 185-188.

Figure Captions

Figure 1. (a) Sketch map of the Iberian Massif showing the Ossa-Morena Zone (OMZ); BCSZ-Badajoz-Córdoba shear zone; CIZ- Central Iberian Zone, CZ- Cantabrian Zone, GTMZ-Galicia- Trás-os-Montes Zone; PLZ- Pulo do Lobo Zone; SPZ- South Portuguese Zone; WALZ- West-Asturian Leonese Zone; (b) Schematic geological map of the Ossa-Morena Zone showing the Évora gneiss dome, and its extension to the Aracena and Lora del Río massifs, and Badajoz-Cordoba shear zone locations. The numbers refer to the ages in millions of years of plutonic rocks (circles and ellipses in white) and of high grade-metamorphic rocks (circles and ellipses in black): geochronological data compiled from Casquet et al. (1998), Montero et al. (2000), Romeo et al. (2006), Pin et al. (2008), Azor et al. (2008), Pereira et al. (2009, 2012, 2015, 2020), Antunes et al. (2011), Lima et al. (2012), Moita et al. (2015), Cambeses et al. (2015), Dias da Silva et al. (2018), and Rodríguez et al., (2022).

Figure 2. Schematic geological section across the Ossa-Morena Zone illustrating the superposition of Variscan contractional D_3 structures on extensional D_2 structures. Location of the cross-section A-B is shown in Fig. 1b.

Figure 3. Geological maps showing the relationships between regional S_2 foliation and the Visean plutonic rocks of: (a) Vale de Maceiras (adapted from Gonçalves et al., 1975) and (b) Campo Maior (adapted from Pinto Coelho and Gonçalves, 1972). See locations in Figure 1b.

Figure 4. Field aspects of the Vale de Maceiras plutonic rocks magmatic foliation: outcrop surface is (a) vertical and (b) horizontal; and the sheared metasedimentary host rocks of the Vale de Maceiras pluton: (c) S_{2b} extensional crenulation cleavage cutting the S_n schistosity, interpreted to represent Variscan D_2 progressive extensional deformation event; (d-e)

intrafoliar folds; (f) S_{2b} extensional crenulation cleavage cutting the S_{2a} foliation and intrafolial folds.

Figure 5. Photomicrographs of the metasedimentary host rocks of the Vale de Maceiras pluton showing the development of (a) S_{2b} superposed to S_{2a} and S_0 coincided with the growth of biotite mica-fish; microfolds related to S_{2b} axial planar cleavage; (b) S_{2a} foliation coincided with the growth of biotite mica-fish; (c) syn-tectonic andalusite porphyroblast grew relatively late and before concerning S_{2a} and S_{2b}, respectively, (d-e) S_{2b} extensional crenulation cleavage transecting S_{2a} foliation. (d) S_{2b} is defined by the variable percentage of cleavage domains (darker with mica and opaque minerals enrichment) concerning microlithons; (e) andalusite porphyroblasts including S_{2a} foliation are preserved in microlithons. Mineral abbreviations are after Whitney and Evans (2010).

Figure 6. Summary of the petrographic relationships between mineral phases (P) and fabrics (D) in metapelitic and metabasic rocks of the Vale de Maceiras (a) and Campo Maior (b) study areas. A late Devonian age was estimated for the M1 high-pressure event in the Badajoz-Cordoba shear zone (Abati et al., 2018 and references therein). Fabric-porphyroblast nomenclature after Rubenach and Bell (1988) and Passchier and Trouw (2005): P- Mineral; D- Deformation stage; $P \leq Dn$ - Pre- to syn-tectonic; $Dn < P < Dn+1$ - inter-tectonic; $Dn \supset P$- syn-tectonic; $Dn \leq P$- syn- to post-tectonic; (c) Pressure-Temperature diagrams (based on Spear, 1995) for the metapelitic rocks of Vale de Maceiras (green; this study) and Campo Maior (grey; Pereira et al., 2008b; 2010; Abati et al., 2018 and references therein) studied areas, showing the relationship of the thermal increase during the emplacement of Visean mafic-intermediate plutons at different crustal levels, and Variscan extensional D_2 deformation event.

Figure 7. Field aspects of the Campo Maior plutonic rocks and host migmatitic rocks: (a) Orthomigmatite with schlieren oriented parallel to the migmatitic foliation and a sigmoidal-

shape mafic schollen (white arrow) indicating the sense of shear; (b) Orthomigmatite with folded migmatitic foliation cut across by a thin high strain shear zone (white arrow); (c) sharp and diffuse contact of the quartz-diorite with the host orthomigmatite (white arrow); (d) Schlieren in quartz-diorite (white arrow) is local evidence of flow; (e) more leucocratic quartz-diorite in the contact (white arrow) between microdiorite (right) and quartz-diorite (left); (f) oriented mafic minerals (Cpx, Bt) define a magmatic foliation ($S_{mg;}$ white arrow) in the microdiorite.

Figure 8. Optical microphotographs and BSE images showing mineral assemblages and textures from the Vale de Maceiras and Campo Maior mafic-intermediate plutonic rocks (a-f) and the Campo Maior orthomigmatites (g and h) rocks. Mineral abbreviations after Whitney and Evans (2010).

Figure 9. Geochemical classification diagrams for samples of plutonic and metamorphic rocks from the Campo Maior and Vale de Maceiras areas. Sanukitoid data compiled by Gómez-Frutos and Castro (2022) are represented by the background Kernel density diagram. Geochemical data from Évora Massif (Alto de São Bento, black crosses; Rodríguez et al., 2022; Moita et al., 2009; 2015) are also included as an example of arc-like compositions and for regional comparison. (a) TAS diagram after Irvine and Baragar (1971) showing all samples plotted in the subalkaline field. (b) SiO_2 vs K_2O diagram by Peccerillo and Taylor (1976) representing all samples following the high K calc-alkaline trend. (c) CaO vs MgO diagram from Castro (2021) revealing the relationship between the calc-alkaline cotectic (black dashed line) and sanukitoid cotectic (black line) series according to Gómez-Frutos and Castro (2022). (d) Or-An-En diagram with the sanukitoid series as a Kernel density plot, and the relationship between calc-alkaline cotectic (black dashed line) and sanukitoid cotectic (black line) series; all samples are plotted close to the sanukitoid series. Projection is addressed by the algebraic

transformation of oxide components (SiO_2, TiO_2, Al_2O_3, FeO, MgO, MnO, CaO, Na_2O, K_2O) into a new base defined by Or, An, Opx, Qz, Crn, Ilm, Ab, Mt, and the exchange vector FeMn-1. (e) Pearce's diagram (Pearce et al., 1984), where almost all rocks plot in the field of volcanic arc granites (VAG). Grey dots in (a-d) correspond to representative samples of other mafic-intermediate plutonic rocks compiled from Vale Maceira and Campo Maior areas (Pinto Coelho and Gonçalves, 1972; Lopes, 2004; Lains Amaral, 2017), used for comparison.

Figure 10. REE chondrite normalized (Nakamura, 1974) diagrams for the plutonic and metamorphic rocks from the Campo Maior and Vale de Maceiras areas.

Figure 11. Concordia diagrams showing the U-Pb data for zircon of the high-K mafic-intermediate plutonic rocks of the Ossa-Morena Zone: (a) Vale de Maceiras orthopyroxene-gabbro; (b) Campo Maior orthopyroxene-microdiorite; and (c) Campo Maior quartz-diorite. Error ellipses are drawn at 2-sigma.

Figure 12. (a) Schematic 3D-model illustrating the syn-tectonic emplacement of the Vale de Maceiras and Campo Maior plutonic rocks (D_2-M_2 stage; ca. 340-330 Ma), when flat-lying planar structures were formed; (a_1) The space for the emplacement of the Vale de Maceiras pluton was probably created at a dilatational jog contemporaneous with the S_{2a} foliation developed in a Variscan D_2 extensional shear zone, later overprinted by a C' shear zone (a_2); The Vale Maceiras plutonic rocks show a magmatic foliation parallel to S_{2b} extensional crenulation cleavage suggesting an interplay between magmatic and tectonic stresses during pluton emplacement (a_2); (b) Schematic 3D-model showing overprinting of Variscan D_3 contractional deformation event (D3-M3 stage; ca. 315-300 Ma), causing folding, thrusting and wrenching of earlier D_2 structures. (b_1) Simplified geological map of the Vale de Maceiras pluton and the structures observed in the host metasedimentary rocks, when they experienced tilting; (b_2) The Campo Maior plutonic rocks are intruded in sheared migmatites; Folds

developed on a migmatitic pre-existing foliation in internal domains of sigmoidal-shape domains (including a metamafic boudin); folds showing rotation of hinges at the margin of high-strain shear zone (mylonitic gneiss); Photomicrograph of a quartz-feldspathic gneiss with mylonitic foliation defined by biotite, sillimanite (enlargement of a D_2 high-strain shear zone); Mylonitic foliation show anastomosing geometries and locally the foliations show variable dips due to folding and tilting.

Figure 13. Schematic 3D-model illustrating pluton emplacement, extensional deformation, metamorphism, synorogenic sedimentation, and volcanism at Visean in the Ossa-Morena Zone. Geochronological data is compiled from [1] Pereira et al., (2009), [2] Rodríguez et al., 2022; [3] Dias da Silva et al., (2018); [4] Pereira et al., (2015); [5] Moita et al., 2015; [6] Antunes et al. (2011); and [7] Pereira et al. (2020).

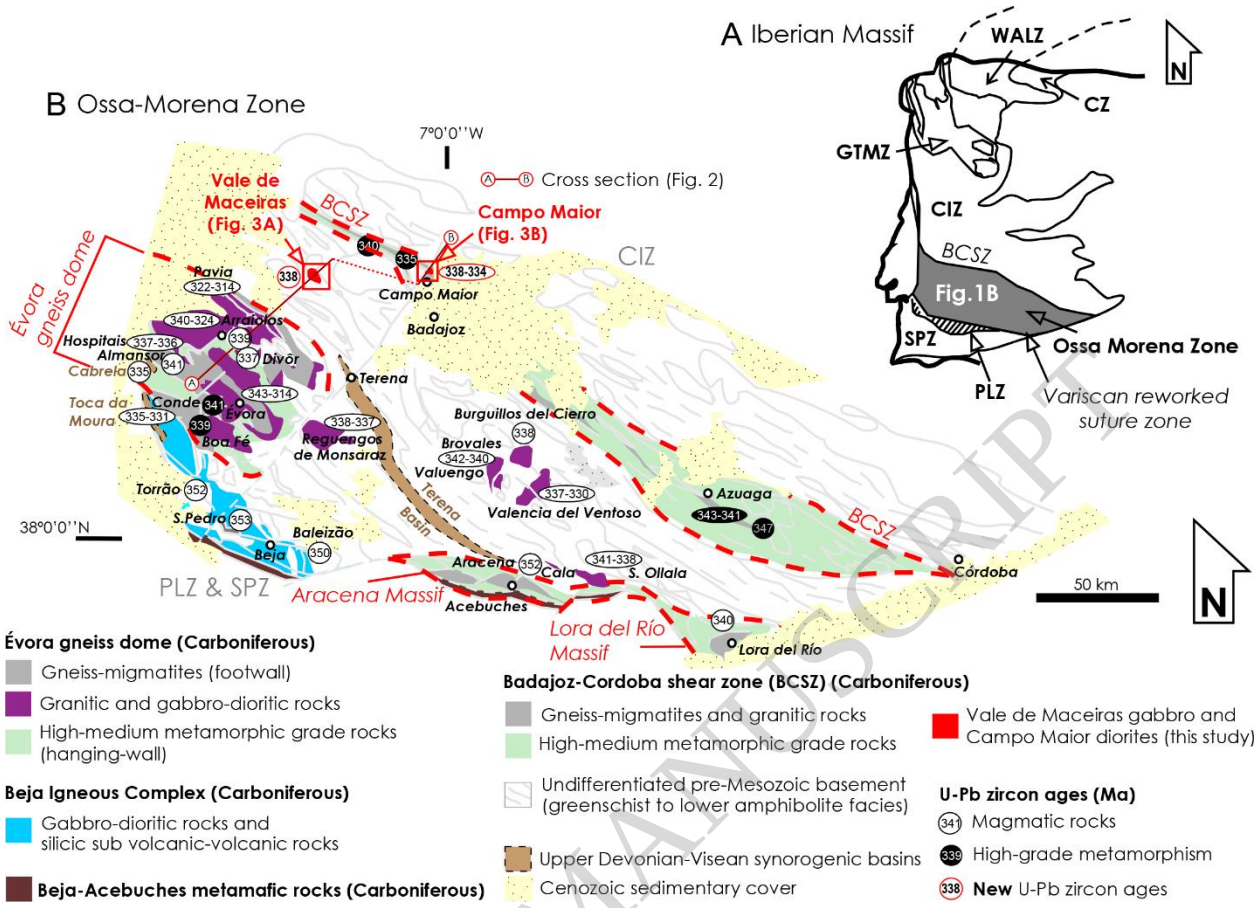

Figure 1

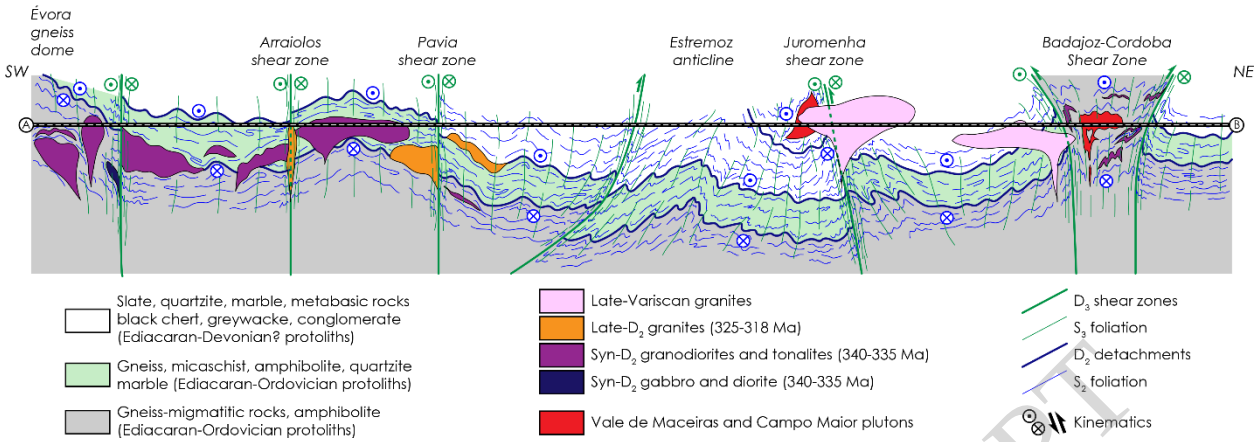

Figure 2

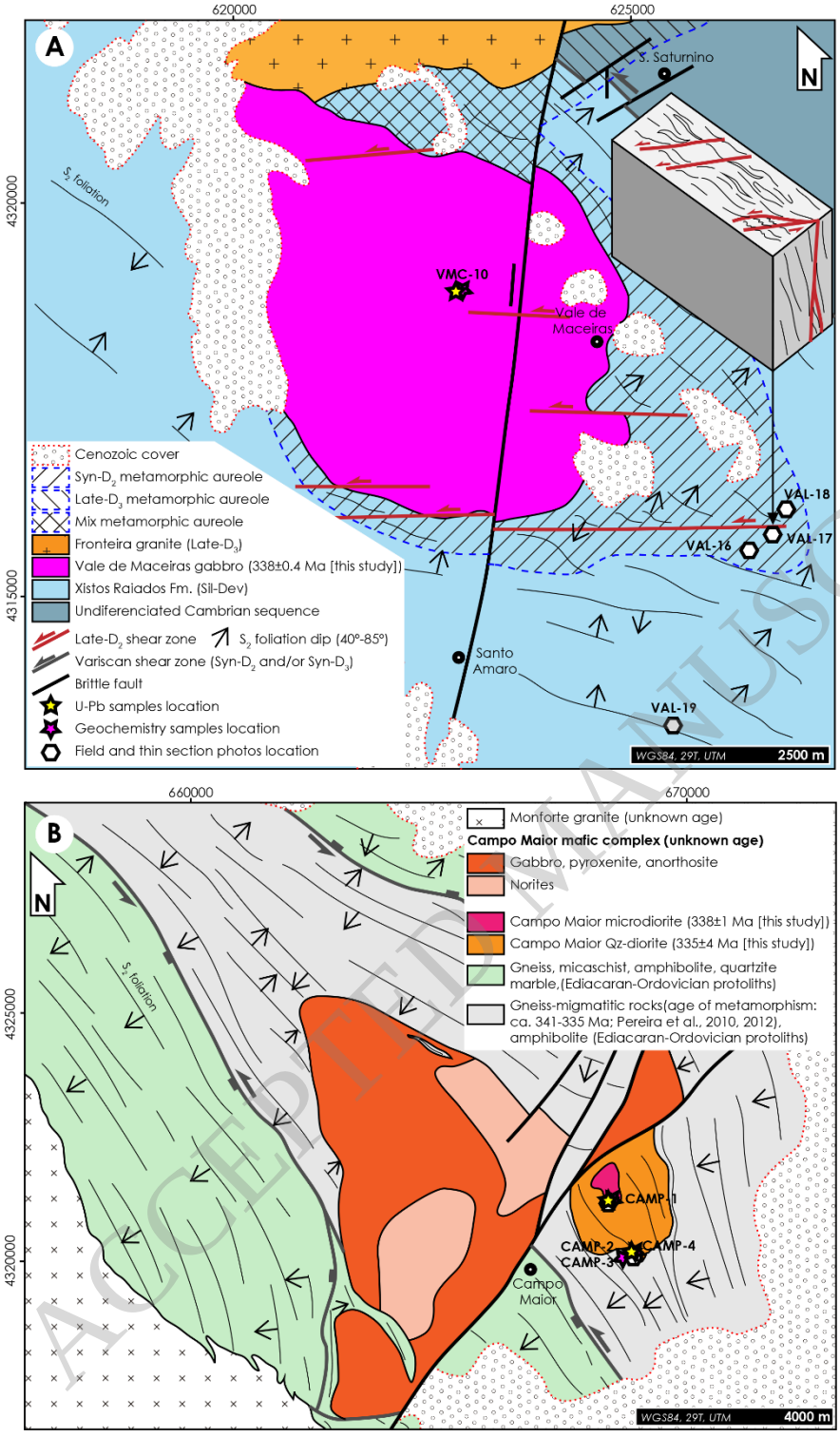

Figure 3

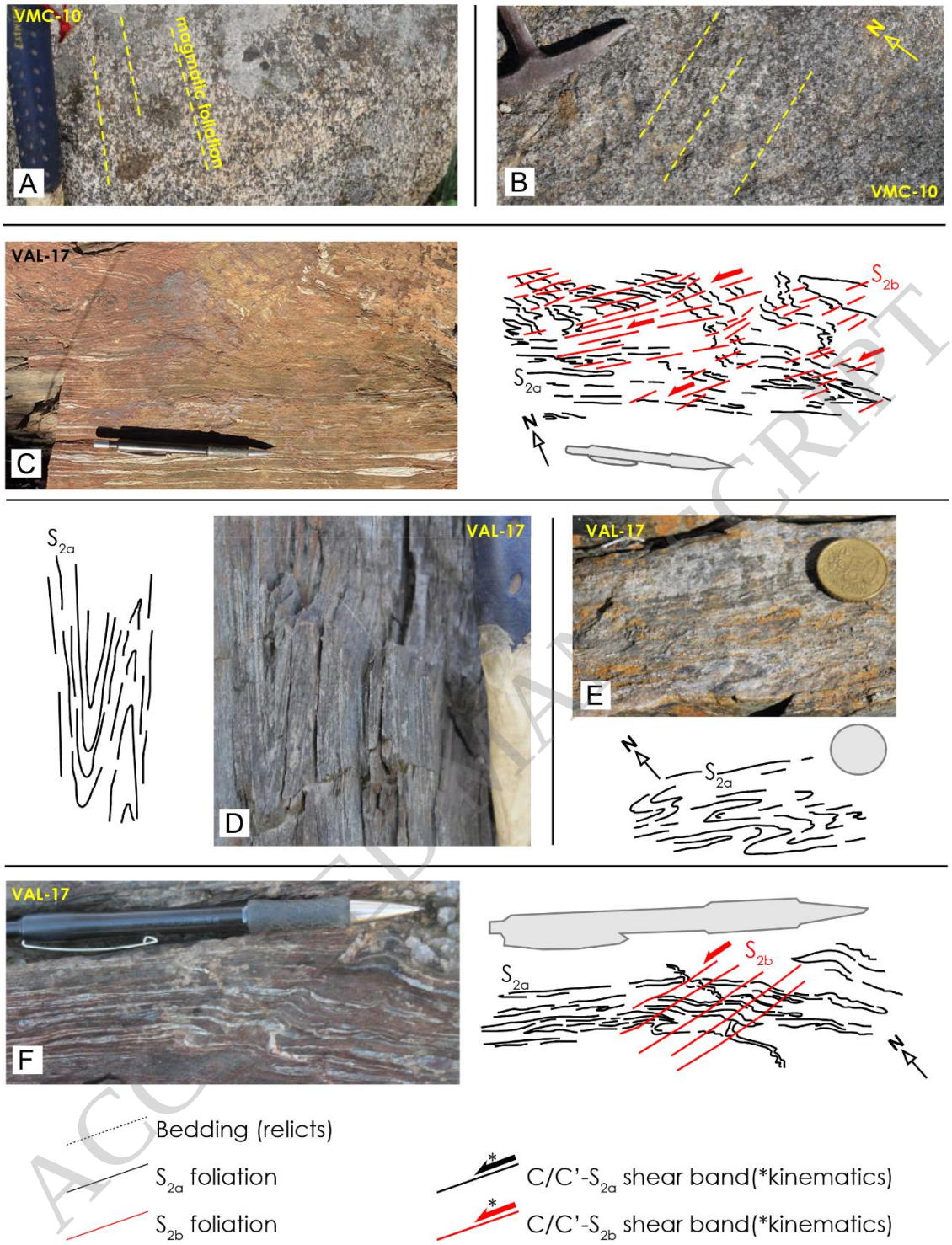

Figure 4

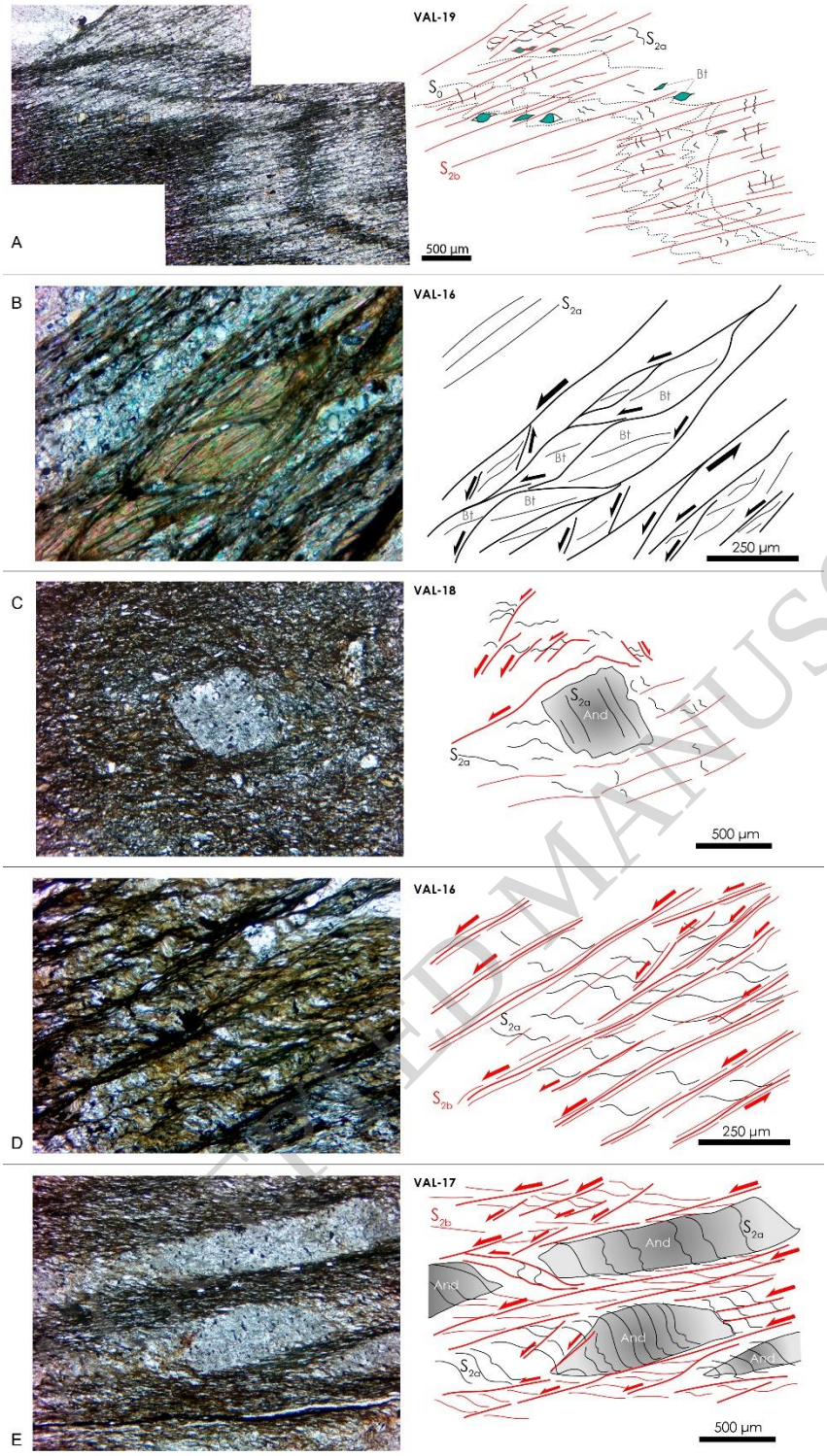

Figure 5

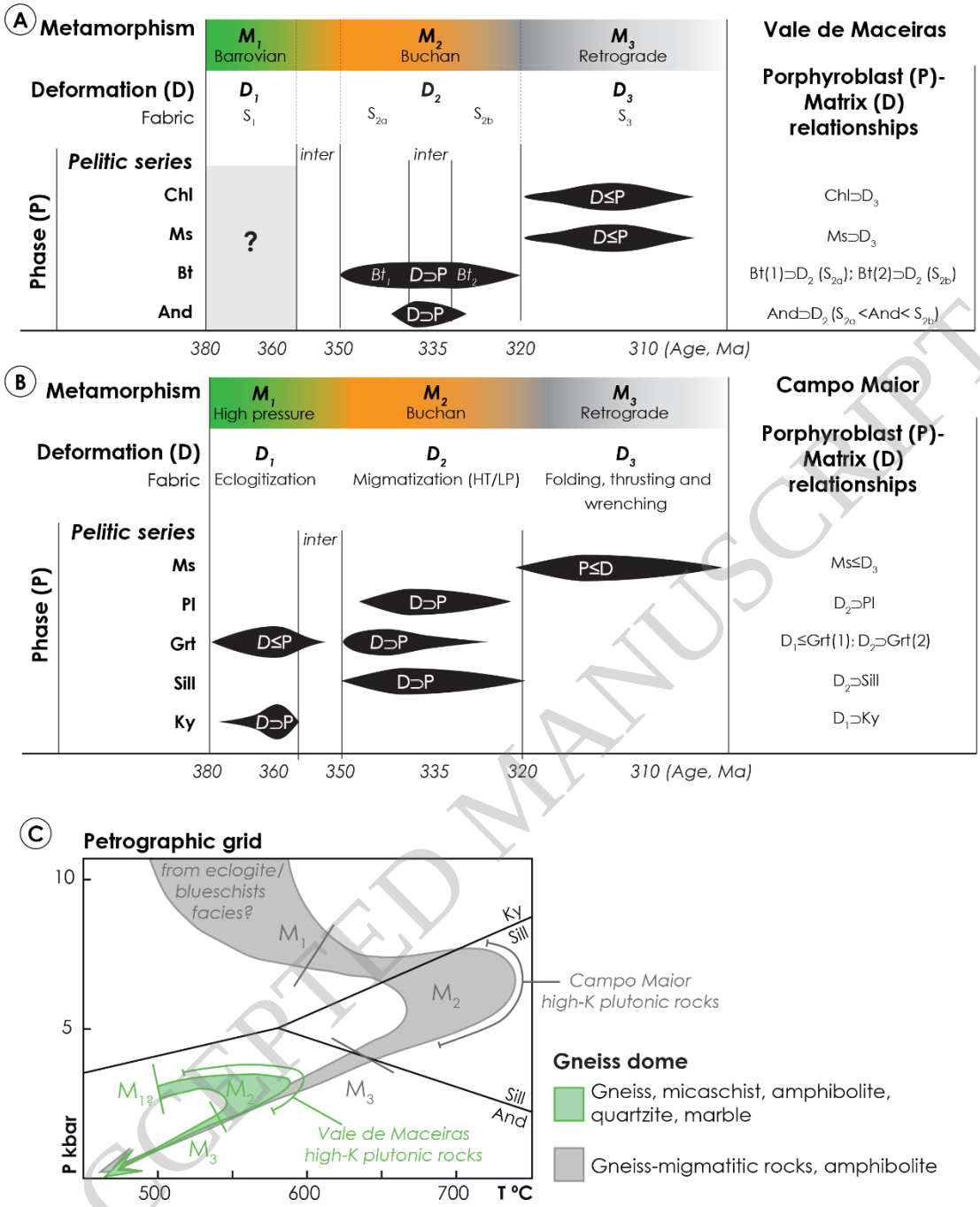

Figure 6

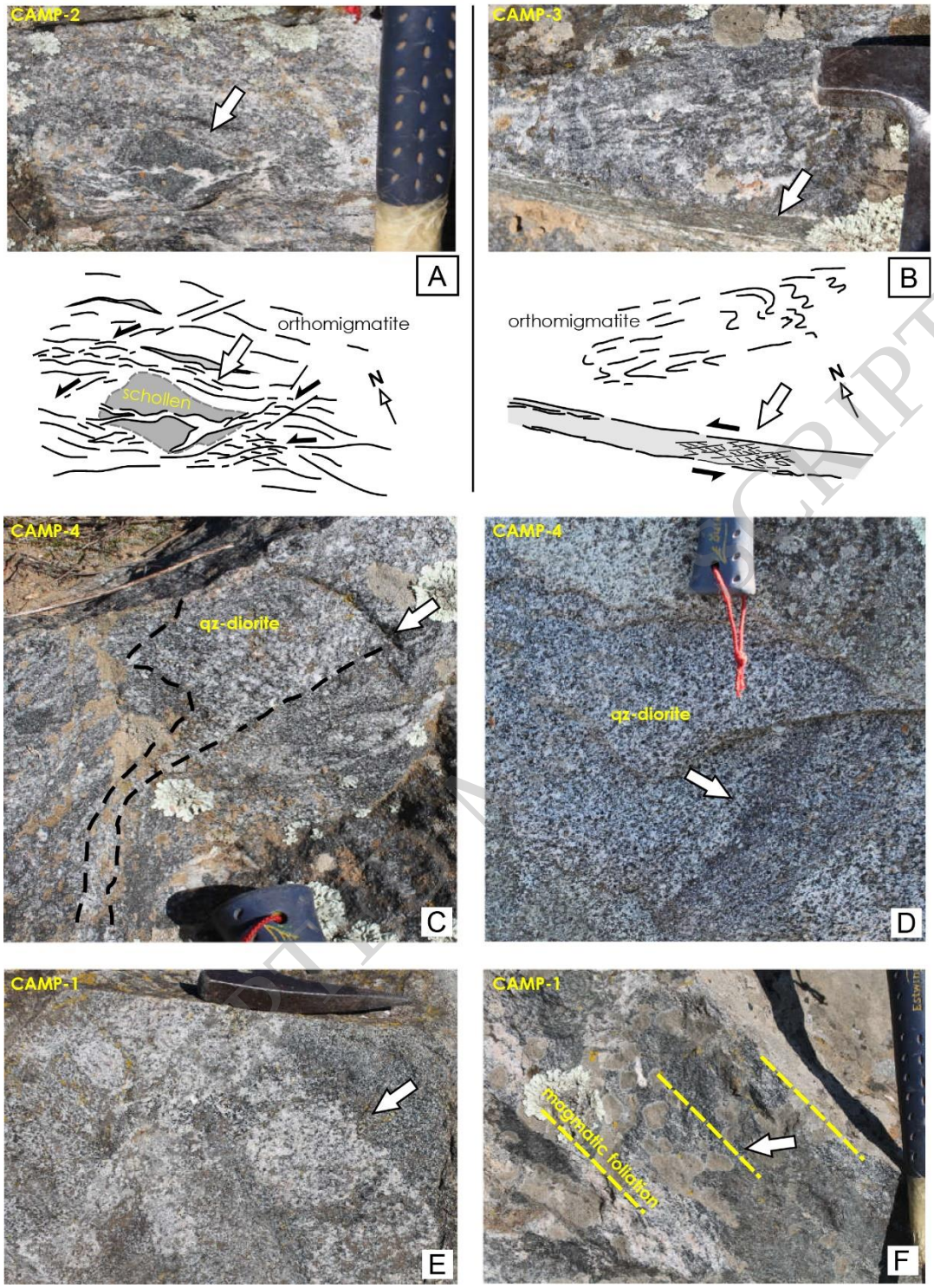

Figure 7

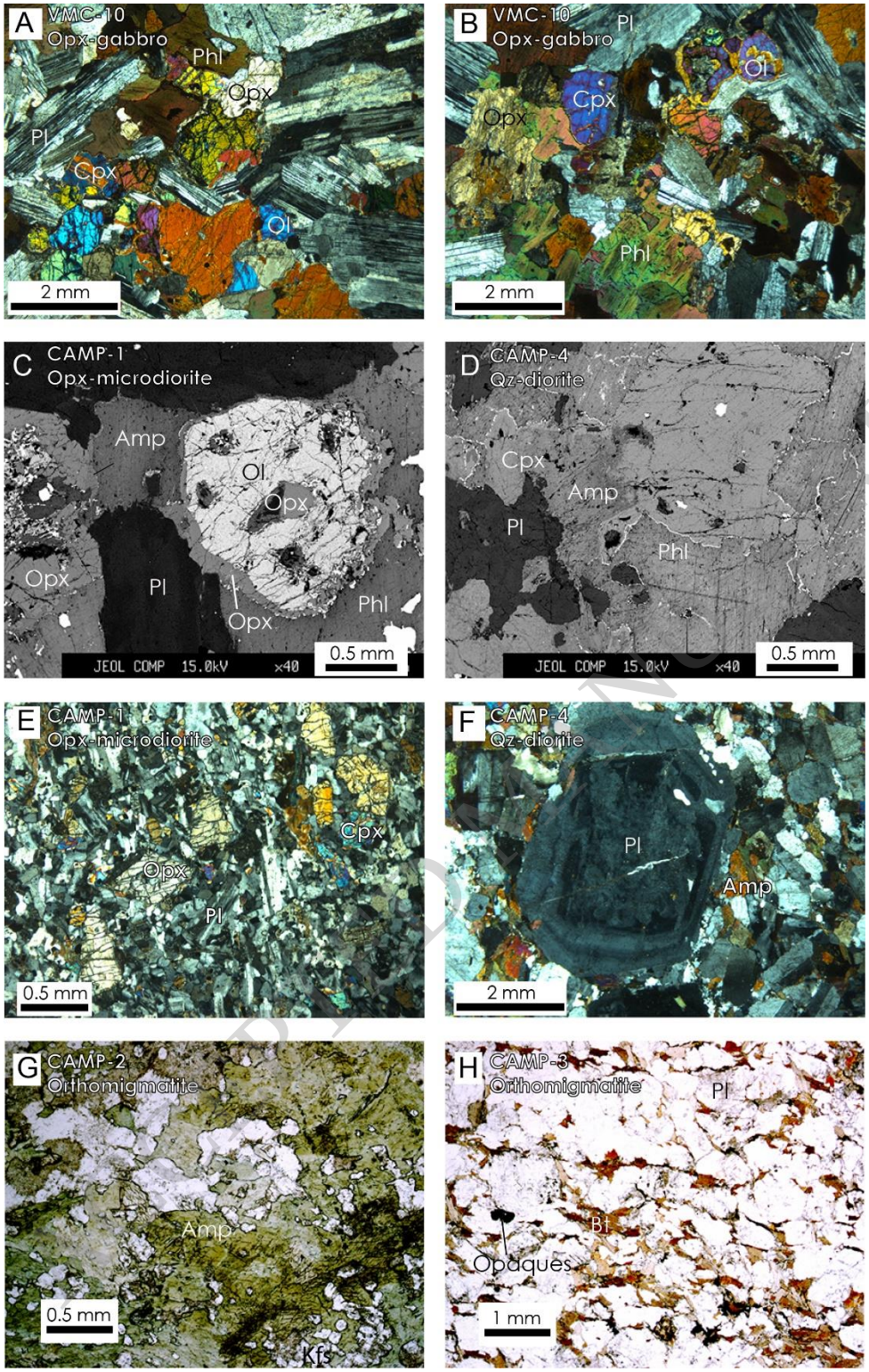

Figure 8

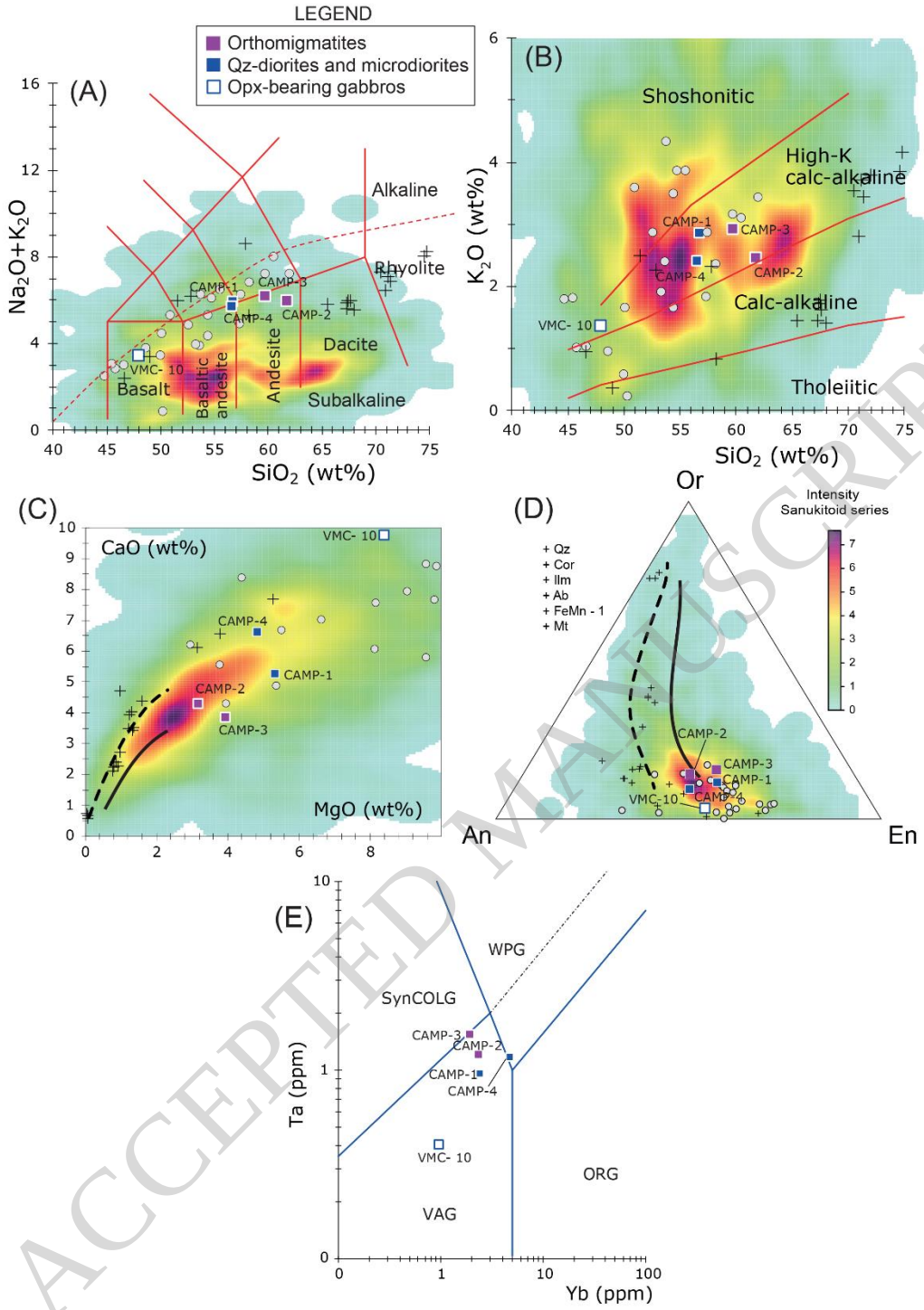

Figure 9

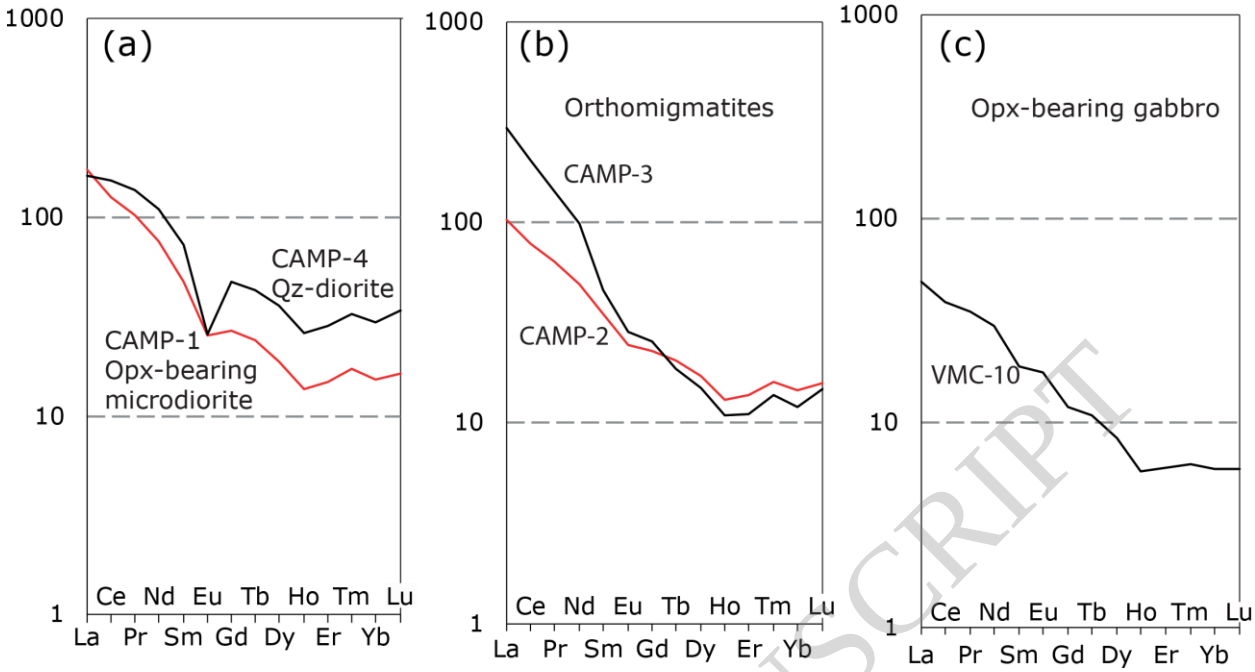

Figure 10

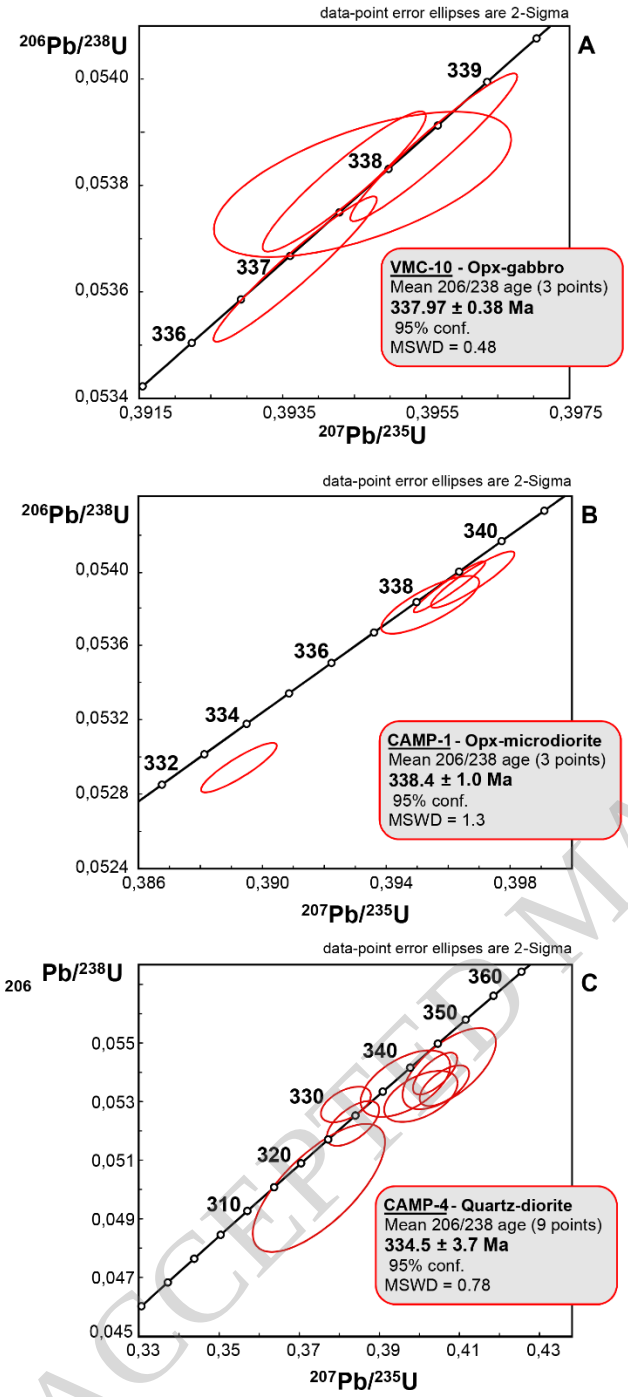

Figure 11

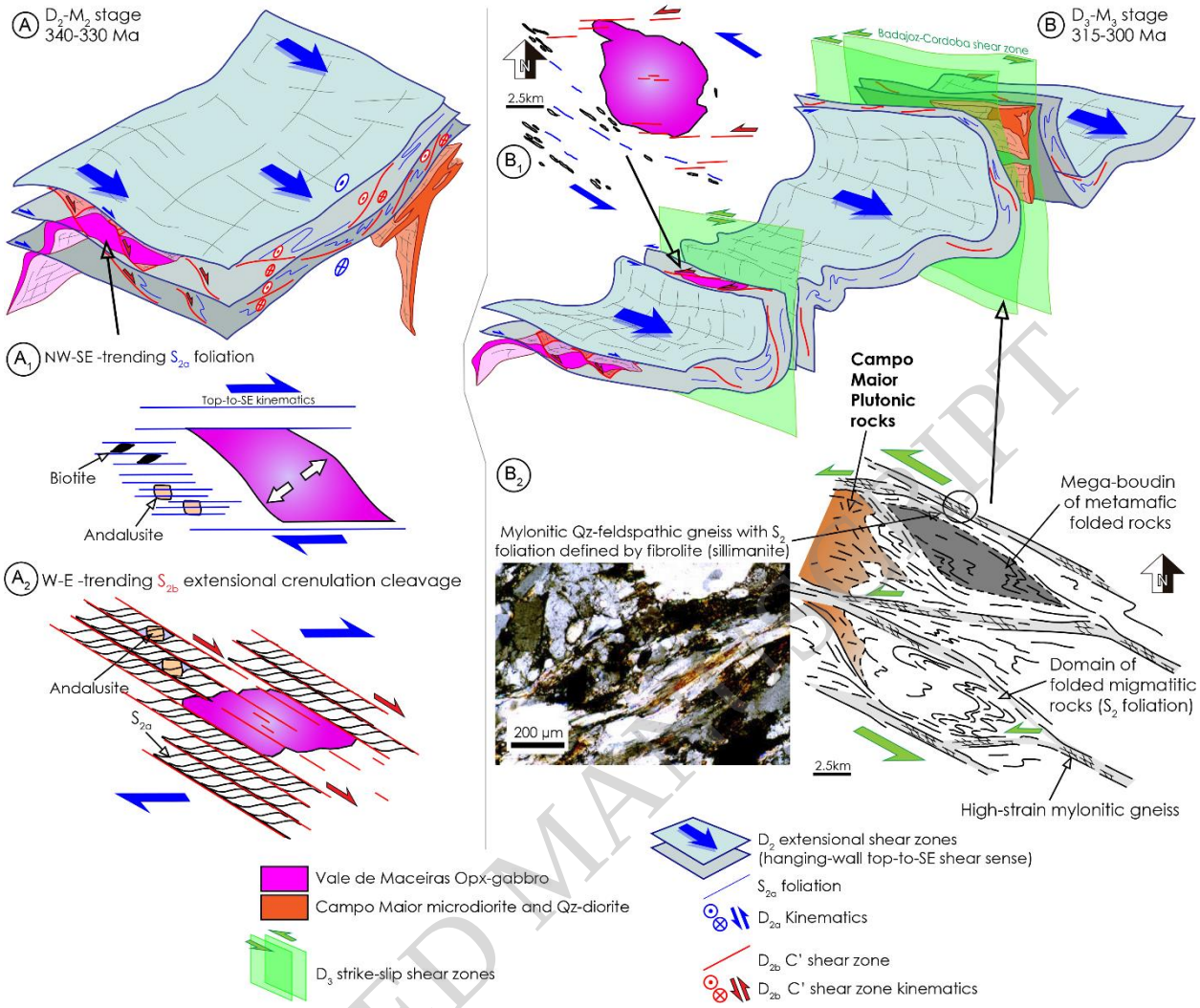

Figure 12

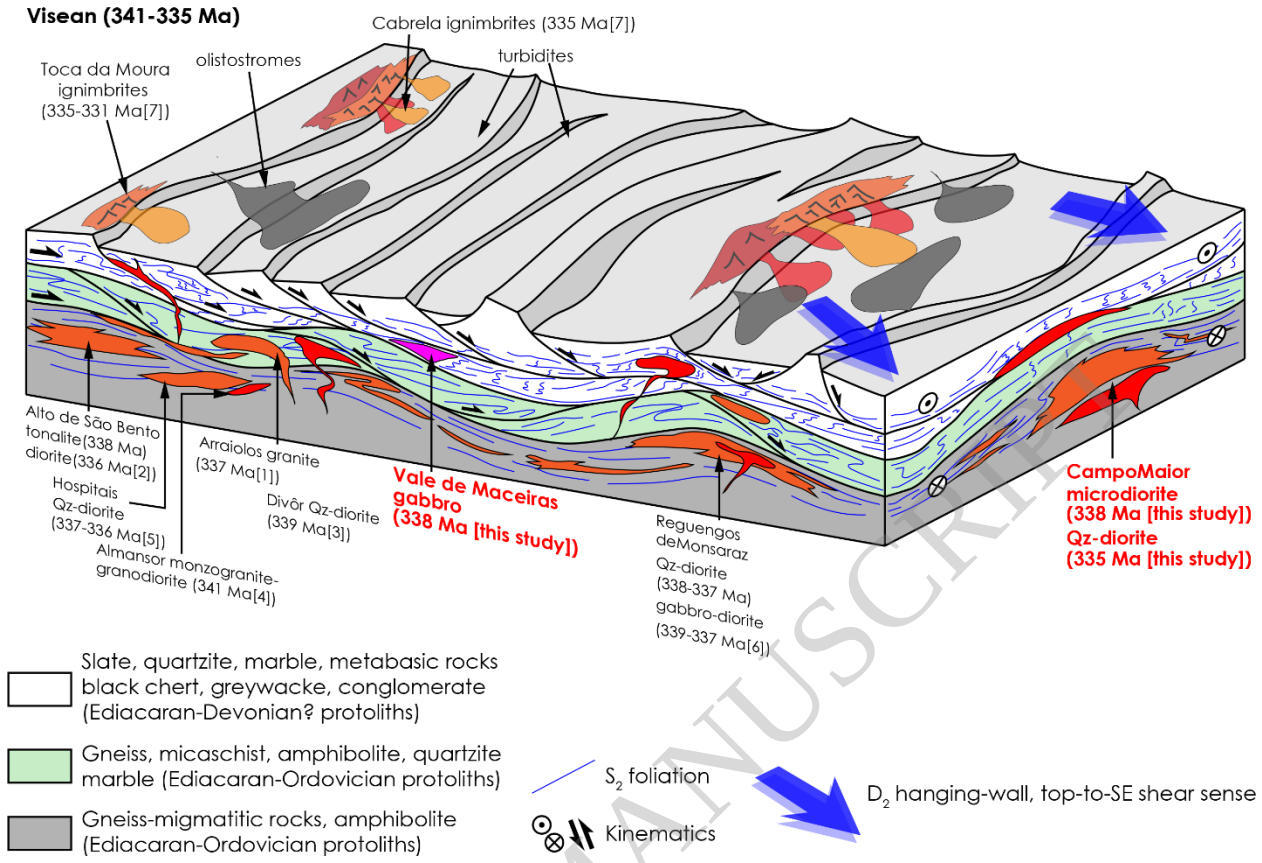

Figure 13